International Journal of Bifurcation and Chaos, Vol. 20, No. 7 (2010) 2045–2070

DOI: 10.1142/S0218127410026927

DEGENERATE BIFURCATIONS AND BORDER COLLISIONS IN PIECEWISE SMOOTH 1D AND 2D MAPS

IRYNA SUSHKO
Institute of Mathematics,
National Academy of Sciences of Ukraine
Kyiv School of Economics, Kyiv, Ukraine

LAURA GARDINI
Department of Economics and Quantitative Methods,
University of Urbino, Italy

Received October 28, 2009; Revised December 2, 2009

We recall three well-known theorems related to the simplest codimension-one bifurcations occurring in discrete time dynamical systems, such as the fold, flip and Neimark–Sacker bifurcations, and analyze these bifurcations in presence of certain degeneracy conditions, when the above mentioned theorems are not applied. The occurrence of such degenerate bifurcations is particularly important in piecewise smooth maps, for which it is not possible to specify in general the result of the bifurcation, as it strongly depends on the global properties of the map. In fact, the degenerate bifurcations mainly occur in piecewise smooth maps defined in some subspace of the phase space by a linear or linear-fractional function, although not necessarily only by such functions. We also discuss the relation between degenerate bifurcations and border-collision bifurcations.

Keywords: Border collision; piecewise smooth; degenerate bifurcations.

1. Introduction

The present work contributes to the study of bifurcations occurring in *discrete* dynamical systems defined by *continuous nonsmooth* functions. This research argument is of wide interest nowadays due to applied problems arising in different fields of science when some real process characterized by sharp switching is modeled by piecewise smooth functions. In fact, many works on piecewise smooth (PW for short) dynamical systems have been motivated by the study of models describing particular electrical circuits, systems for the transmission of signals, etc. (see, e.g. [Maistrenko *et al.*, 1993, 1995; Banerjee & Grebogi, 1999; Banerjee *et al.*, 2000a, 2000b; Feely *et al.*, 2000; Fournier-Prunaret *et al.*, 2001; Halse *et al.*, 2003; Avrutin & Schanz, 2006; Zhusubaliyev *et al.*, 2006]). The PW smooth models are used in several context also in economics and other social sciences (see [Gallegati *et al.*, 2003; Puu & Sushko, 2002, 2006; Sushko *et al.*, 2003, 2005, 2006; Gardini *et al.*, 2008; Tramontana *et al.*, 2008]). For other relevant examples coming from engineering, physics, biology, economics and other fields, we refer to the books by Zhusubaliyev and Mosekilde [2003], di Bernardo *et al.* [2008] and the references therein.

The bifurcation theory for smooth systems is quite well developed, while for PW smooth systems it is still far from being complete. The main point is that besides the standard bifurcations (either local or global) well-studied for smooth maps, the bifurcation theory of PW smooth maps must deal

with new dynamic phenomena, related to the existence of borders in the phase space, or so-called switching manifolds, in which the function defining the system changes, and thus has discontinuous Jacobian. An invariant set of the PW smooth map may collide with such a border, and this collision may lead to a bifurcation often followed by drastic changes such as, for example, direct transition from an attracting fixed point to a chaotic attractor. All the new bifurcation phenomena related to the border collisions are nowadays collected under the term *Border Collision Bifurcations* (BCB for short). First introduced in Nusse and Yorke [1992] (see also [Nusse & Yorke, 1995]), this term is now commonly used. However, we have to mention also earlier works by Leonov [1959] and Feigin [1970] describing quite powerful methods to study bifurcation phenomena in PW smooth systems. The works by Feigin (in which the related bifurcation is called C-bifurcation), came to wide knowledge only recently due to the republication and elaboration of his main results in [di Bernardo *et al.*, 1999], while the works by Leonov are still mainly unknown (in [Gardini *et al.*, 2009b; Avrutin *et al.*, 2009b] the Leonov's method is effectively improved and applied to the study of BCB in a one-dimensional PW linear discontinuous map).

The actual state of the art in the understanding of the BCB is such that the only well established field is the classification of the BCB occurring in one-dimensional (1D for short) *continuous* PW smooth maps (as we shall recall in Sec. 3), while for 2D PW smooth maps only the simplest cases are classified (see [Banerjee *et al.*, 2000b]). Indeed, the BCB in 1D and 2D PW smooth continuous maps can be classified according to the parameters of the related *normal forms* first proposed in [Nusse & Yorke, 1992, 1995]. Namely, the 1D BCB normal form is the well-known *skew-tent map* whose dynamics are completely described (see, e.g. [Maistrenko *et al.*, 1993]), while in the 2D case the normal form is a 2D PW linear map given by two linear functions (see Sec. 4), which possesses quite rich and complicated dynamics not yet well investigated (see [Banerjee & Grebogi 1999; Zhusubaliyev *et al.*, 2006; Sushko & Gardini 2008; Simpson & Meiss 2008; Gardini *et al.*, 2009a; Avrutin *et al.*, 2009a]). Note that the well-known Lozi map [Lozi, 1978] is a special case of the 2D BCB normal form.

While studying the bifurcation sequences in PW linear maps, particular bifurcations are observed and described by several authors, related to the eigenvalues of some cycle crossing the unit circle: For example, an eigenvalue of the attracting cycle crossing -1 may not lead to an attracting cycle of double period, as it occurs in smooth maps, but to a two-piece cyclical chaotic attractor (it occurs, for example, in the skew-tent map for certain parameter values, as we shall recall in Sec. 3.1). Such a bifurcation is related to the BCB of this chaotic attractor given that it appears exactly at the border in which the map changes its definition. One more relevant example is the so-called *center bifurcation*, first described in [Sushko *et al.*, 2003], occurring in a 2D PW linear map when a pair of complex eigenvalues of an attracting focus crosses the unit circle: For such a map the Neimark–Sacker bifurcation theorem is not applied and, as a result, an invariant closed curve is not born in the neighborhood of the fixed point (in Sec. 4.2, we recall what can be the result of a center bifurcation and, in particular, we present an example of a cyclical chaotic attractor born due to the center bifurcation). It is clear that the absence of the period-doubling cascade in a PW linear map, as well as other nonstandard bifurcations occurring when the eigenvalues cross the unit circle, can be explained by certain degeneracy of linear functions, so that the well-known flip-, fold- and Neimark–Sacker bifurcation theorems are not applied. But indeed not only in PW linear maps such particular bifurcations are observed (see, e.g. [Gardini *et al.*, 2008] where a 1D power-hyperbolic map is considered, while a 2D PW smooth example is given in [Fournier *et al.*, 2008]). So, among others, the following questions arise: What kind of degeneracy leads to the nonstandard local bifurcations related to the eigenvalues crossing the unit circle? How can we classify the results of such bifurcations?

The aim of the present paper is to partially answer the above questions. In Sec. 2, we recall the flip-, fold- and Neimark–Sacker bifurcation theorems and show which conditions are not fulfilled in the case of linear and linear-fractional maps. Then we define *Degenerate Bifurcations* for generic PW smooth maps. In Sec. 3, we illustrate the occurrence of degenerate bifurcations in 1D PW smooth maps via three different examples: First, we recall the dynamics of the well-known skew-tent map, then we consider a 1D PW smooth map defined by linear and logistic functions, and then one more map defined by power and linear-fractional functions. In particular, we show how the degenerate bifurcations may lead to cyclical chaotic intervals of period 2^k

for any integer $k \geq 0$, as well as how the skew-tent map is used to classify the BCB in 1D PW smooth maps. In Sec. 4, we consider 2D PW linear map which is the normal form to study BCB in 2D PW smooth maps. For this map, we describe the degenerate bifurcation of the fixed point leading to cyclical chaotic attractors of period 2^k for any integer $k \geq 0$, and the super- and subcritical center bifurcations. The degenerate bifurcations of an attracting cycle of period 3 are also described.

2. Fold, Flip and Neimark–Sacker Bifurcation Theorems and the Related Degenerate Bifurcations

In this section we recall three well-known theorems giving the conditions for the simplest codimension-one bifurcations occurring in discrete time dynamical systems, such as the fold bifurcation (related to an eigenvalue 1), the flip bifurcation (an eigenvalue -1) and the Neimark–Sacker bifurcation (a pair of complex-conjugate eigenvalues with modulus 1). As usual, we use the maps of the lowest possible dimensions in which the bifurcations listed above can occur, which are 1D maps for the fold and flip bifurcations, and 2D maps for the Neimark–Sacker (NS for short) bifurcation, also known as Hopf bifurcation for maps, or secondary Hopf bifurcation. This is not a loss of generality because these results can be applied to an n-dimensional system by using the related center manifold theorems (for details we refer to [Guckenheimer & Holmes, 1983], or [Kuznetsov, 1998]).

So, let us consider a one-parameter family $f_\mu : \mathbb{R} \to \mathbb{R}$ of 1D maps. Assume that f_μ has a fixed point x_0 and let $f'_\mu(x_0) = \lambda(\mu)$. We formulate the fold and flip bifurcation theorems following Guckenheimer and Holmes [1983]; see also [Sharkovsky *et al.*, 1997].

Fold bifurcation theorem. *Let $f_\mu : \mathbb{R} \to \mathbb{R}$ be a one-parameter family of C^2-maps depending smoothly on the parameter μ. Let x_0 be a fixed point of f_μ and $\lambda(\mu_0) = 1$. If at $\mu = \mu_0, x = x_0$*

(1) $(d^2/d^2x) f_{\mu_0}(x_0) = f''_{\mu_0}(x_0) > 0$ *and*
(2) $(d/d\mu) f_{\mu_0}(x_0) < 0$

then there exist $\varepsilon > 0$ and $\delta > 0$ such that for $\mu \in (\mu_0 - \delta, \mu_0)$ the map f_μ has no fixed points in the interval $(x_0 - \varepsilon, x_0 + \varepsilon)$, and for $\mu \in (\mu_0, \mu_0 + \delta)$ the map f_μ has two fixed points (one attracting and one repelling) in the interval $(x_0 - \varepsilon, x_0 + \varepsilon)$.

The theorem remains true if the signs of both inequalities (1) and (2) are reversed, while if only one sign is changed then the fixed points appear at decreasing μ.

Recall that there are two more bifurcations associated with the eigenvalue $\lambda(\mu_0) = 1$[1]: The *pitchfork* bifurcation, occurring when condition (1) of the above theorem becomes $f''_{\mu_0}(x_0) = 0$, leads from one attracting (respectively repelling) fixed point, to three fixed points, one repelling and two attracting (respectively one attracting and two repelling). The *transcritical* bifurcation, occurring when condition (2) of the above theorem becomes $(d/d\mu) f_{\mu_0}(x_0) = 0$ is related to two fixed points, one attracting and one repelling, existing for $\mu \in (\mu_0 - \delta, \mu_0 + \delta)$, which merge at $\mu = \mu_0$ and exchange their stability.

For a 1D linear map,[2] say $f_\mu : x \mapsto \mu x + b$ with $\mu > 0$, the condition (1) of the above theorem is not satisfied, as we have $f''_\mu(x) = 0$ not only at the fixed point (as it occurs in the pitchfork bifurcation), but in the whole region of definition. At the bifurcation value $\mu = 1$ one can distinguish between two cases:

(1) for $b = 0$ (a proper linear map) $f_\mu(x)|_{\mu=1} = x$, that is any point $x \in \mathbb{R}$ is fixed; The fixed point $x_0 = 0$ just changes its stability when μ passes through 1.
(2) for $b \neq 0$ (an affine map) f_μ has no real fixed point, as $x_0 = b/(1-\mu)|_{\mu=1} = \infty$. If we include in our considerations the second fixed point of f_μ located at infinity then this bifurcation can be seen as a particular kind of the *transcritical* bifurcation: When μ passes through 1 we have an exchange of stability between these two fixed points.

So, it follows that for a linear map the result of the bifurcation associated with the eigenvalue $+1$ is trivial, but considering some attracting k-cycle of a PW smooth map f_μ, the same bifurcation (with eigenvalue $+1$) may occur, as the related

[1]We recall that the normal form for these bifurcations are as follows: $x' = x + \mu - x^2$ (fold); $x' = x(1+\mu) - x^2$ (transcritical); $x' = x(1+\mu) - x^3$ (pitchfork).

[2]We remark that in this paper we call *linear map* what is more properly an *affine map*, as it is almost of standard use in the theory of dynamical systems.

map f_μ^k may satisfy in suitable intervals the condition $f_\mu^k(x) = x$ (as in the first case above), and one can observe quite complicated dynamics as a consequence of this bifurcation. In Sec. 3 we shall give an example of a 1D PW smooth unimodal map defined by linear and logistic functions, in which the bifurcation associated with the eigenvalue +1 can lead to cyclical chaotic intervals of period 2^k where $k \geq 0$ can be any integer (depending on the parameter of the logistic map).

We can consider also the case in which a PW smooth map f_μ has a fixed point $x_0(\mu)$ which tends to infinity as $\lambda(\mu)$ tends to 1 (as in the second case related to the linear map; obviously it may occur also in 1D nonlinear maps). As we shall see in Sec. 4, this occurs for cycles of the 2D BCB normal form, points of which tend to infinity as one of the eigenvalues tends to 1 (other examples can be found in [Sushko & Gardini, 2008; Avrutin *et al.*, 2009a]).

So, we can introduce the following *definitions* of degenerate bifurcations related to the eigenvalue 1: The first one (DB1 for short) refers to fixed points which are in the real phase space at the bifurcation value, while the second one, Degenerate Transcritical Bifurcation (DTB for short), refers to fixed points which are at infinity at the bifurcation value.

Let $f_\mu : \mathbb{R} \to \mathbb{R}$ be a one-parameter family of 1D PW smooth maps depending smoothly on the parameter μ, and $\lambda(\mu) = f'_\mu(x_0(\mu))$ at a fixed point x_0.

Degenerate Bifurcation 1 (DB1). *Let $\delta > 0$ be such that for $\mu \in (\mu_0 - \delta, \mu_0 + \delta)$ the fixed point x_0 of the map f_μ is not a break point, and $\lambda(\mu_0) = 1$. Then the fixed point x_0 of f_μ undergoes the degenerate bifurcation DB1 when the eigenvalue $\lambda(\mu)$ crosses 1 as μ crosses μ_0 and $f_{\mu_0}(x) = x \,\forall\, x \in I, I$ being a suitable interval including x_0.*

It is clear that the interval I in the above definition is bounded either by break points, or their proper images, or I can be unbounded from one side.

Degenerate Transcritical Bifurcation (DTB). *If the fixed point $x_0(\mu)$ tends to infinity and its eigenvalue $\lambda(\mu)$ tends to 1 as μ tends to μ_0, then a DTB occurs as μ crosses μ_0.*

We turn now to the

Flip bifurcation theorem. *Let $f_\mu : \mathbb{R} \to \mathbb{R}$ be a one-parameter family of C^3-maps depending smoothly on the parameter μ; let x_0 be a fixed point of $f_\mu, \lambda(\mu) = f'_\mu(x_0(\mu))$ and $\lambda(\mu_0) = -1$. If at $\mu = \mu_0, x = x_0$*

(1) $(d^3/d^3x)f^2_{\mu_0}(x_0) < 0$ *and*
(2) $(d/d\mu)f'_{\mu_0}(x_0) < 0$,

then there exist $\varepsilon > 0$ and $\delta > 0$ such that for $\mu \in (\mu_0 - \delta, \mu_0)$ the map f_μ has exactly one fixed point in the interval $(x_0 - \varepsilon, x_0 + \varepsilon)$ and this fixed point is attracting; while for $\mu \in (\mu_0, \mu_0 + \delta)$ the map f_μ has a repelling fixed point and an attracting 2-cycle in the interval $(x_0 - \varepsilon, x_0 + \varepsilon)$.

This theorem describes the *supercritical* (or "soft") flip bifurcation, while if one changes the sign of (1) and replaces the word "attracting" by "repelling" and vice versa, then the theorem describes the *subcritical* (or "sharp") flip bifurcation. As for the inequality (2), changing its sign the 2-cycle appears for decreasing values of μ. So, to get the flip bifurcation (super- or subcritical) at $\mu = \mu_0, x = x_0$, the following conditions have to be satisfied: $\lambda(\mu_0) = -1, (d^3/d^3x)f^2_{\mu_0}(x_0) \neq 0$ and $(d/d\mu)f'_{\mu_0}(x_0) \neq 0$.

Note that in the proof of this theorem (see for example in [Sharkovsky *et al.*, 1997]), it becomes evident that the condition in (1) $(d^3/d^3x)f^2_{\mu_0}(x_0) \neq 0$ is equivalent to $Sf_\mu \neq 0$ where $Sf = (f'''/f') - (3/2)(f''/f')^2$ is the Schwarzian derivative of f (where it is understood evaluated at $\mu = \mu_0$ and $x = x_0$).[3] Moreover, it is possible to see that $Sf(x) = 0 \,\forall\, x$ iff f is linear or linear-fractional[4] (see, e.g. [De Melo & van Strien, 1993]), and for such maps the condition $Sf_\mu(x) \neq 0$ is not satisfied not only at a fixed point, but in the whole region of definition. Thus the bifurcation related to an eigenvalue equal to -1 for linear and linear-fractional maps does not lead to the appearance of a cycle of double period (attracting or repelling). This fact is quite obvious for the 1D linear map: For $f_\mu : x \mapsto \mu x + b$ at $\mu = -1$ any point $x \in \mathbb{R}$, except for the fixed point $x_0 = b/(1 - \mu)$, is periodic of period 2, while for $\mu < -1$ the trajectory of any point $x \neq x_0$ is divergent.

[3]This condition corresponds to that of the parameter a in Theorem 3.5.1 in [Guckenheimer & Holmes, 1983], in fact it is easy to see that $a = -Sf/3$ at $\mu = \mu_0$ and $x = x_0$.

[4]A linear-fractional map, also called *real Möbius transformation* [De Melo & van Strien, 1993], and *Riccati difference equation with constant coefficients* [Kocic & Ladas, 1993], is given by $y' = (ay + b)/(cy + d)$ where a, b, c, d are real numbers such that $(bc - ad) \neq 0, c \neq 0$.

To see the result of the considered bifurcation in a 1D linear-fractional map $g : y \mapsto (ay+b)/(cy+d), bc-ad \neq 0, c \neq 0$ in which, without loss of generality, we consider $c > 0$, we first note that it is topologically conjugate to the map $f : x \mapsto k/x+\mu$ (via the homeomorphism $h(x) = x/\sqrt{c} - d/c$ and $k = (bc-ad)/\sqrt{c}, \mu = (a+d)/\sqrt{c}$). The fixed points of the map f are $x_{1,2} = (\mu \pm \sqrt{\mu^2+4k})/2$, which are real for $\mu^2+4k > 0$. The eigenvalues of f at $x = x_{1,2}$ are $\lambda = -k/x_{1,2}^2$, and $\lambda = -1$ occurs only for $\mu = 0$. So, at the bifurcation value we have $f : x \mapsto k/x$, moreover, $f^2 : x \mapsto x$ for any $k \neq 0$ and $x \neq 0$, i.e. any point $x \in \{\mathbb{R}/0\}$ is 2-periodic, except for the fixed points $x_{1,2} = \pm\sqrt{k}$. For $k > 0$ the map f has two real fixed points $x_{1,2}$, one attracting and one repelling, existing for any μ, which exchange their stability at the bifurcation value $\mu = 0$ (note that the fold bifurcation cannot occur for $k > 0$). Just for completeness, let us comment also the dynamics of $f(x)$ for $k < 0$: For $|\mu| < 2\sqrt{|k|}$ the map f has no real fixed points, and the points $x \in \mathbb{R}$ either are all periodic, of the same period (which depends on μ and k), or all are quasiperiodic, with a trajectory dense in $\mathbb{R}$ [Kocic & Ladas, 1993; Sushko & Gardini, 2009]. In particular, at $\mu = 0$ any point is 2-periodic. At $\mu = \pm 2\sqrt{|k|}$ the fixed points $x_{1,2}$ undergo the standard fold bifurcation, followed by two real fixed points $x_{1,2}$, one attracting and one repelling, existing for any μ in the range $|\mu| > 2\sqrt{|k|}$.

Coming back to the bifurcation related to $\lambda = -1$, we have seen that for linear and linear-fractional maps this bifurcation is characterized by infinitely many 2-cycles at the bifurcation value, and it gives rather trivial results after the bifurcation. But dealing with a PW linear or PW smooth map f_μ (with components not necessarily all linear or linear-fractional, as we shall see in the examples in Sec. 3), then for some k-cycle (fixed point of the kth iterate of the map) the same bifurcation may occur, with eigenvalue $\lambda = -1$, and in this case what occurs after is not trivial (and clearly depends on the global shape of the function): It can give rise to several quite complicated dynamics. This motivates our *definition*:

Degenerate Flip Bifurcation (DFB for short). *Let $f_\mu : \mathbb{R} \to \mathbb{R}$ be a one-parameter family of piecewise C^3-smooth maps depending smoothly on the parameter μ; Let x_0 be a fixed point of $f_\mu, \delta > 0$ be such that for $\mu \in (\mu_0 - \delta, \mu_0 + \delta)$ the fixed point x_0 is not a break point of f_μ and $\lambda(\mu_0) = f'_{\mu_0}(x_0(\mu_0)) = -1$. At $\mu = \mu_0$ a degenerate flip bifurcation occurs if*

(1) $Sf_{\mu_0}(x) = 0 \, \forall \, x$ *in a neighborhood of* x_0 *and*
(2) $(d/d\mu) f'_{\mu_0}(x_0) \neq 0$.

Stated in other words, we say that a k-cycle of a PW smooth 1D map f_μ undergoes a DFB when no point of the cycle coincides with any of the break points of $f_\mu, \lambda(\mu)$ crosses -1 as μ crosses μ_0 and at the bifurcation value the map f_μ^k is locally (in suitable interval) linear or linear-fractional. Note that we have immediately a necessary and sufficient condition: A k-cycle of a PW smooth map f_μ undergoes a DFB iff at the bifurcation value ($\lambda = -1$) the map f_μ^k has *locally* (in a neighborhood of the related fixed points) infinitely many 2-cycles. Moreover, in analogy with what occurs in smooth maps, if a k-cycle of a PW smooth map f_μ undergoes a DFB then the same k-cycle of the map f_μ^{2k} undergoes a DB1, as *locally* (in suitable intervals) the map satisfies $f_\mu^{2k}(x) = x$.

Clearly it is also possible to have the degenerate analogues of a *supercritical* or *subcritical* flip bifurcation but, as we shall see from the examples in Sec. 3.1, the dynamic effects associated with a DFB may be of many different kinds.

The three degenerate bifurcations defined above may clearly occur in higher-dimensional maps associated with one eigenvalue which crosses ± 1, as we shall see in the examples in Sec. 4. In such cases, the conditions given above refer to the center manifold, and the dynamic effect clearly depends also on the other eigenvalues and on the global definition of the map.

Let us consider now a family of 2D maps $F_\mu : \mathbb{R}^2 \to \mathbb{R}^2$ and formulate the Neimark–Sacker (or secondary Hopf) bifurcation theorem following Guckenheimer and Holmes [1983]:

Neimark–Sacker bifurcation theorem. *Let $F_\mu : \mathbb{R}^2 \to \mathbb{R}^2$ be a one-parameter family of 2D maps which has a smooth family of fixed points $x(\mu)$ at which the eigenvalues are complex conjugated $\lambda(\mu), \overline{\lambda}(\mu)$. Assume*

(1) $|\lambda(\mu_0)| = 1$, *but* $\lambda^j(\mu_0) \neq 1$ *for* $j = \overline{1,4}$;
(2) $(d/d\mu)(|\lambda(\mu_0)|) = d \neq 0$.

Then there is a smooth change of coordinates H so that the expression $HF_\mu H^{-1}$ in polar coordinates has the form

$HF_\mu H^{-1}(r,\theta) = (r(1 + d(\mu-\mu_0) + ar^2), \theta + c + br^2)$ *+ higher-order terms.*

If, in addition,

(3) $a \neq 0$,
then there is a 2D surface Σ (*not necessarily infinitely differentiable*) *in* $\mathbb{R}^2 \times \mathbb{R}$ *having quadratic tangency with the plane* $\mathbb{R}^2 \times \{\mu_0\}$ *which is invariant for* F_μ. *If* $\Sigma \cap (\mathbb{R}^2 \times \{\mu_0\})$ *is larger than a point, then it is a simple closed curve.*

For the explicit expression of the coefficient a in (3) we refer to [Guckenheimer & Holmes, 1983] (see also [Kuznetsov, 1998]). The signs of the coefficients d and a determine the direction and stability of the bifurcating orbits, while c and b give information on the rotation numbers. In particular, similarly to the flip bifurcation case, the NS bifurcation can be supercritical (or "soft", when $a < 0$) and subcritical (or "sharp", when $a > 0$). We remark that numerically it is possible to deduce which kind of bifurcation occurs just from the local behavior of the fixed point at the bifurcation value: If the fixed point is locally attracting (respectively repelling), then the NS bifurcation is supercritical (respectively subcritical). Notice that when $a = 0$ the theorem cannot be applied.

For 2D linear maps the condition $a \neq 0$ is obviously not satisfied, and, again, not only at the fixed point, but in the whole region of definition of the map. Indeed, considering a linear map, say, $F_\mu : \mathbb{R}^2 \to \mathbb{R}^2$, with complex-conjugate eigenvalues $\lambda(\mu), \overline{\lambda}(\mu)$, if $|\lambda(\mu_0)| = 1$ then the fixed point $x_0(\mu_0)$ of F_μ is a *center*, so that the phase plane is filled with invariant ellipses having center in $x_0(\mu_0)$ and the trajectory of any point $x \neq x_0(\mu_0)$ belongs to one of such ellipses, on which it can be either periodic, or quasiperiodic, depending on the rotation number, rational or irrational, respectively (i.e. depending on the parameters). For $\mu \neq \mu_0$ the fixed point is either a globally attracting focus, or a repelling focus and the trajectory of any point $x \neq x_0(\mu)$ spirals away and goes to infinity. However, as commented for the previous bifurcations, in the case of a 2D PW smooth map with some linear components we may have locally the same kind of dynamic behavior, so that we are led to the following *definition*:

Center bifurcation. *Let* $F_\mu : \mathbb{R}^2 \to \mathbb{R}^2$ *be a one-parameter family of 2D PW smooth maps which has a smooth family of fixed points* $x_0(\mu)$ *at which the eigenvalues are complex conjugated* $\lambda(\mu), \overline{\lambda}(\mu)$, *and let* $|\lambda(\mu_0)| = 1$. *We say that the fixed point undergoes a center bifurcation at* $\mu = \mu_0$ *if* $x_0(\mu_0)$ *is locally a center.*

Clearly we can have the same bifurcation for a k-cycle of a 2D PW smooth map F_μ when the cycle is not at a BCB and the fixed points of F_μ^k undergo the center bifurcation, so that at $\mu = \mu_0$ in suitable neighborhoods of the fixed points of F_μ^k the phase space is filled with closed invariant curves.

The center bifurcation was first described in Sushko *et al.* [2003] (see also [Sushko & Gardini, 2008]) to indicate a bifurcation occurring in a 2D PW linear map when the complex conjugate eigenvalues at the fixed point cross the unit circle, and it was shown that such a bifurcation has analogies with the Neimark–Sacker bifurcation: Namely, as in a supercritical bifurcation, a pair of cycles can appear due to the bifurcation, one attracting and one saddle, and the unstable set of the saddle cycle, approaching points of the attracting cycle, forms a closed invariant attracting curve (and similar analogue exists with the subcritical case, leading to a repelling closed invariant curve). Differently from the smooth case such a curve is a piecewise linear set (generally made up by an infinite number of segments, which may be finite in number only in a particular kind of noninvertibility of the map). After the bifurcation value the closed curve does not appear in a neighborhood of the fixed point or cycle, but at a finite distance from it (depending on the distance of the cycle from the boundary separating the regions of different definitions of the map).

In Sec. 4 we give examples of the center bifurcation occurring in 2D PW linear maps. We shall see that besides the appearance of attracting closed curves, due to a supercritical center bifurcation (analogue of a supercritical NS bifurcation) we can have also a subcritical center bifurcation (analogue of a subcritical NS bifurcation), when a repelling closed curve surrounds the stable focus cycle. Also we shall see that as a consequence of a center bifurcation we may have a direct transition to a chaotic attractor.

To end this section it is worth to mention the codimension-two bifurcations occurring when the nondegeneracy conditions are not satisfied (at a fixed point), such as the cusp bifurcation, the generalized flip bifurcation, and the Chenciner, or generalized NS, bifurcation: See [Kuznetsov, 1998] for the details and additional conditions which have to be fulfilled. These bifurcations are not related to the degenerate bifurcations we are interested in, as described in this work, because the additional conditions require nonzero derivatives of order larger then 2. Moreover, for such bifurcations

the nondegeneracy conditions are not satisfied only at the fixed point, and not in an open subset of the phase space, as in case of the degenerate bifurcations.

Summarizing, we have shown that for linear 1D and 2D maps the nondegeneracy conditions of the theorems recalled above are not satisfied, as well as the nondegeneracy condition (1) of the flip bifurcation theorem for the 1D linear-fractional maps, and these conditions fail not only at the fixed points, but in the whole region of definition of the related maps. As a consequence, the results of the transition of the eigenvalues through unit circle are trivial, while these results can be not trivial at all when dealing with PW smooth maps whose fixed points or cycles undergo the degenerate bifurcations described above.

3. Examples of Degenerate Bifurcations in 1D PW Smooth Maps

In this section we present three examples of 1D PW smooth unimodal maps in which the degenerate bifurcations can occur leading to different dynamic behaviors. As a first example, we consider the well-known skew-tent map which is a 1D PW linear map defined by two linear functions. We recall that the DFB of an attracting k-cycle, $k \geq 3$, of the skew-tent map leads to $2k$-cyclical chaotic intervals, the DFB of the 2-cycle results in 2^i-cyclical chaotic intervals, where $i \geq 2$ can be any integer depending on parameters; while the fixed point of the skew-tent map can undergo a subcritical or supercritical period-doubling DFB, or its DFB can lead to 2^i-cyclical chaotic intervals, $i \geq 1$. As a second example we consider a PW map given by linear and logistic functions, fixed point of which can undergo the DB1 leading to 2^i-cyclical chaotic intervals, $i \geq 1$. The third map is interesting as an example of 1D PW smooth map in which the degenerate bifurcations are associated with nonlinear components (not only with linear and linear-fractional functions). In the second and third examples we show also how the dynamic behavior of the skew-tent map is important in the theory of BCB, given that it is used as a 1D BCB normal form.

3.1. *1D BCB normal form (skew-tent map)*

Consider a 1D PW linear map f given by two linear functions and defined as

$$f : x \mapsto f(x) = \begin{cases} f_L(x) = \alpha x + \varepsilon, & x \leq 0, \\ f_R(x) = \beta x + \varepsilon, & x \geq 0, \end{cases} \quad (1)$$

where α, β and ε are real parameters.

Due to the linearity the map f has the following scaling property: $f(kx, \alpha, \beta, k\varepsilon) = kf(x, \alpha, \beta, \varepsilon)$ for any $k > 0$, so that if in the phase space the map f has an invariant (bounded) set, it shrinks to 0 as $\varepsilon \to 0$. This also implies that for $k = 1/|\varepsilon|, \varepsilon \neq 0$, with the change of variable $y = x/|\varepsilon|$ we are led to a map in the same form as in (1), where $\varepsilon = -1$ or $\varepsilon = 1$. However, in order to determine all the possible bifurcation curves, it is enough to consider only one of the two cases, say $\varepsilon = -1$, as the bifurcation curves associated with the second case $\varepsilon = 1$ can be obtained by a symmetry property. In fact, the map $x \mapsto f(x, \alpha, \beta, \varepsilon)$ is topologically conjugate with $y \mapsto f(y, \beta, \alpha, -\varepsilon)$ through $y = -x$, so that the bifurcation structure of the (α, β)-parameter plane for $\varepsilon = 1$ is symmetric with respect to the line $\alpha = \beta$ to the one for $\varepsilon = -1$. We emphasize that for any fixed $\varepsilon < 0$ the bifurcation diagram in the plane (α, β) is the same as for $\varepsilon = -1$, and similarly for any fixed $\varepsilon > 0$ the bifurcation diagram in the plane (α, β) is the same as for $\varepsilon = 1$ (symmetric with respect to the line $\alpha = \beta$ to the one obtained for $\varepsilon = -1$, which means that in the equations of the bifurcation curves it is enough to exchange α with β and vice versa).

So, let $\varepsilon < 0$. It is shown in Fig. 1 the partition of the (α, β)-parameter plane into the regions having qualitatively the same dynamic for the map f. If one considers the parameter range $\alpha < 0, \beta > 0$ then the map f is called *skew-tent map* (or *tent map* if $\alpha = -\beta$), possessing quite rich dynamics which was intensively studied by many authors (see, e.g. [Ito *et al.*, 1979; Takens, 1987; Maistrenko *et al.*, 1993; Nusse & Yorke, 1995]).

Let us describe in detail the bifurcation structure of the (α, β)-parameter plane for $\alpha < 0, \beta > 0$. The point $x = 0$ is the point of minimum and the absorbing interval I is given by $I = [f(0), f^2(0)] = [\varepsilon, \varepsilon(\alpha + 1)]$. For $\beta < 1$ the map f has a unique fixed point $x^*_L = \varepsilon/(1 - \alpha) < 0$, which is globally attracting for $\alpha > -1$ and repelling for $\alpha < -1$, while for $\beta > 1$ the map f has one more fixed point $x^*_R = \varepsilon/(1 - \beta)$ which is repelling. For $\alpha > -1, \beta > 1$, the basin of attraction of x^*_L is given by $(-\infty, x^*_R)$. When the fixed point x^*_L is unstable then the interval (x^*_{R-1}, x^*_R) is the basin of attraction of the absorbing interval I, which exists as long as $f^2(0) = \varepsilon(\alpha + 1) < x^*_R$. The curve

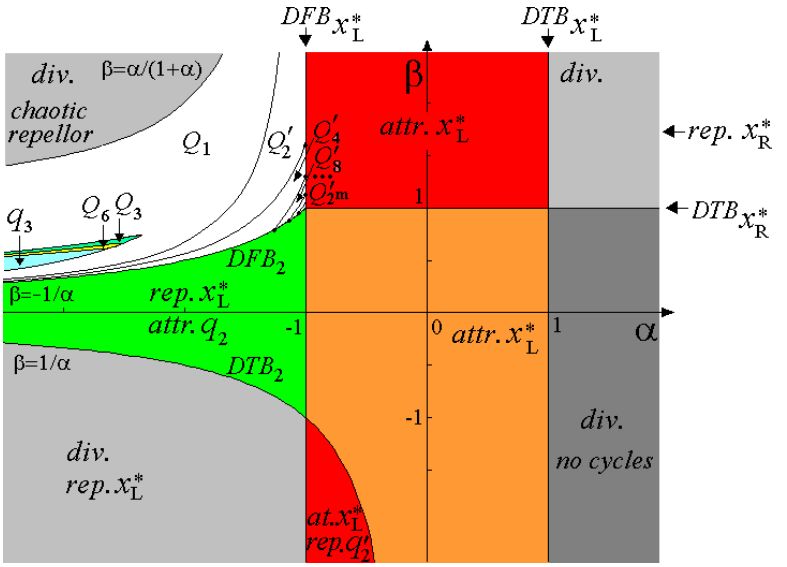

Fig. 1. The partition of the (α, β)-parameter plane into regions having qualitatively the same dynamics for the map f at $\varepsilon < 0$.

$\varepsilon(\alpha+1) = x^*_R$, that is $\beta = \alpha/(1+\alpha)$, corresponds to the contact bifurcation,[5] or boundary crises, leading (for $\beta > \alpha/(1+\alpha)$) to divergence of the generic trajectory of f, so that we are led to consider the parameter range

$$P = \left\{(\alpha, \beta) : \alpha < 0, 0 < \beta < \frac{\alpha}{1+\alpha}\right\}.$$

Depending on the parameters α and β the map f for $(\alpha, \beta) \in P$ can have an attracting cycle q_k of any period $k \geq 2$, as well as cyclical chaotic intervals Q_k of any period $k \geq 1$. In [Maistrenko *et al.*, 1993] the analytical expressions are given for the boundaries of the regions in the (α, β)-parameter plane related to such attractors. In particular, the cycles having period $k \geq 3$ appear in pair, one stable q_k and one unstable q'_k. In order to find the periodic points of such cycles, we proceed as follows. We know that a periodic point $x_1^{k,s}$ of the cycle q_k is obtained by solving the following equation: $f_R^{k-1} \circ f_L(x_1^{k,s}) = x_1^{k,s}$ which leads to the point

$$x_1^{k,s} = \frac{\varepsilon}{1-\alpha\beta^{k-1}} \frac{1-\beta^k}{1-\beta}, \qquad (2)$$

while a periodic point $x_1^{k,u}$ of the cycle q'_k is obtained by solving the following equation: $f_R^{k-2} \circ f_L^2(x_1^{k,u}) = x_1^{k,u}$ which leads to the point

$$x_1^{k,u} = \frac{\varepsilon}{1-\alpha^2\beta^{k-2}} \frac{\alpha\beta^{k-2}(1-\beta)+1-\beta^{k-1}}{1-\beta}, \qquad (3)$$

and the BCB occurs when the periodic point $x_1^{k,u}$ collides with the border, $x_1^{k,u} = 0$, that is for:

$$\alpha = -\frac{1-\beta^{k-1}}{(1-\beta)\beta^{k-2}}. \quad \mathrm{BC}_k \qquad (4)$$

Thus Eq. (4) gives the BCB curve denoted BC_k crossing which a pair of cycles appear, one attracting cycle q_k (a periodic point of which is given in (2)) and a repelling cycle q'_k (a periodic point of which is given in (3)) for $\alpha < \alpha_k$, where α_k is defined below, while both cycles are repelling if $\alpha > \alpha_k$. The eigenvalue of the stable cycle q_k is given by $\lambda = \alpha\beta^{k-1}$ so that it loses stability via DFB when

$$\alpha = -\frac{1}{\beta^{k-1}}. \quad \mathrm{DFB}_k \qquad (5)$$

So, denoting by $\Pi(q_k)$ the stability region of the cycle q_k, this region is given by $(\alpha, \beta) \in \Pi(q_k)$ where

$$\Pi(q_k) = \left\{(\alpha, \beta) : -\frac{1}{\beta^{k-1}} \leq \alpha \leq -\frac{1-\beta^{k-1}}{(1-\beta)\beta^{k-2}}\right\},$$

and it is bounded by the two bifurcation curves BC_k and DFB_k given in (4) and (5), which intersect at the point (α_k, β_k), where β_k is the root of the equation $\beta^k - 2\beta + 1 = 0$ in the interval $(0.5, 1)$ and $\alpha_k = -1/\beta_k^{k-1}$.

It has been shown in [Maistrenko *et al.*, 1993] that the DFB of q_k for $k \geq 3$ leads to cyclical chaotic intervals of double period $2k$, denoted by Q_{2k},

[5]Contact between the invariant interval I and its basin of attraction.

so that the transition $q_k \Rightarrow Q_{2k}$ is the result of the DFB of this cycle. The attracting $2k$-cyclical chaotic intervals Q_{2k} exist in the parameter region bounded by the curves $\mathrm{BC}_k, \mathrm{DFB}_k$ (given in (4), (5), respectively) and by the curve denoted H_k related to the first homoclinic bifurcation of the cycle q_k, given by

$$\beta^{2(k-1)}\alpha^3 - \alpha + \beta = 0. \quad H_k \tag{6}$$

So the transition $Q_{2k} \Rightarrow Q_k$ takes place if the parameter point crosses the curve H_k. The attracting k-cyclical chaotic intervals Q_k exist in the parameter region bounded by the curves BC_k, H_k (given in (4), (6), respectively) and by the curve denoted H'_k corresponding to the first homoclinic bifurcation of the cycle q'_k, given by

$$\beta^{k-1}\alpha^2 + \alpha - \beta = 0. \quad H'_k \tag{7}$$

Thus we have the transition $Q_k \Rightarrow Q_1$ if the parameter point crosses the curve H'_k. For example, the lower boundary of the region $\Pi(q_3)$ (see Fig. 1) is the curve BC_3 corresponding to the "saddle-node" BCB which gives birth to the attracting cycle q_3 and the repelling cycle q'_3. The upper boundary of the $\Pi(q_3)$ region is the curve DFB_3 corresponding to the DFB of the attracting cycle q_3 which becomes repelling, leading to 6-cyclical chaotic intervals Q_6. The boundary between the Q_6-region and the Q_3-region is the curve H_3 corresponding to the first homoclinic bifurcation of the cycle q_3, while the upper boundary of the Q_3-region is the curve H'_3 related to the first homoclinic bifurcation of the cycle q'_3 and leading to a one-piece chaotic interval $Q_1 = I = [\varepsilon, \varepsilon(\alpha + 1)]$.

The bifurcation curves are drawn in Fig. 1 by using their analytical expressions, and each curve corresponds to a particular bifurcation. In that portion of the parameter plane only the stability region of the cycle q_3 is observable, but note that in the strip for $\beta \in (0, 0.5)$ all the regions $\Pi(q_k)$ exist where $k \to \infty$ as α tens to $-\infty$. Moreover, all these cycles of period $k \geq 3$ undergo the same bifurcation sequence (at some fixed α and increasing β), that is, the DFB $q_k \Rightarrow Q_{2k}$ is followed by the transitions $Q_{2k} \Rightarrow Q_k \Rightarrow Q_1$.

It is possible to see in Fig. 1 that the DFB of the 2-cycle q_2 is particular. The eigenvalue of q_2 is given by $\lambda = \alpha\beta$ so that the DFB of q_2 occurs at $\beta = -1/\alpha$. Differently from the cycles q_k for $k \geq 3$ described above, the DFB of q_2 may lead to cyclical chaotic intervals of any even period, that is, we can have the transition $q_2 \Rightarrow Q'_{2^m}$, where $m \geq 2$, moreover, $m \to \infty$ as $\alpha \to -1$ and $\beta = -1/\alpha \to 1$. Two contiguous regions Q'_{2^i} and $Q'_{2^{i+1}}$ are separated by the curve corresponding to the first homoclinic bifurcation of the 2^i-cycle given by

$$\alpha^{\delta_{i+1}}\beta^{\delta_i} + (-1)^i(\alpha - \beta) = 0, \quad H_{2^i}$$

where $\delta_m, m = 0, 1, \ldots$, is the solution of the difference equation $\delta_{i+1} = 2\delta_i + (1 + (-1)^i)/2$, $i = 1, 2, \ldots$, with $\delta_0 = 1$ (see [Maistrenko *et al.*, 1993] for the details).

As the parameter point $(\alpha, \beta) = (-1, 1)$ is an accumulation point for the regions related to the 2^m-cyclical chaotic intervals Q'_{2^m} as $m \to \infty$, we can see that crossing through $\alpha = -1$ the DFB of the fixed point x^*_L may also lead to any one of such 2^m-cyclical chaotic intervals Q'_{2^m} for any $m \geq 1$, while for $-1 < \beta < 1$ the DFB of x^*_L leads to the cycle q_2.

For clarity of exposition, let us comment on the 1D bifurcation diagram obtained for $\beta = 0.5, \varepsilon = -1$ and $\alpha \in [-4.8, -0.95]$, shown in Fig. 2. At $\alpha = -1$ (the DFB of the fixed point x^*_L) each point of the segment $[-1, 0]$ (except x^*_L) is 2-periodic for the map f. This bifurcation gives rise to the attracting 2-cycle q_2. The DFB of q_2 occurs at $\alpha = -1/\beta|_{\beta=0.5} = -2$ and at this bifurcation value there are two segments, $[f(0), f^3(0)]$ and $[0, f^2(0)]$, each point of which (except q_2) is 4-periodic for the map f. The DFB of the cycle q_2 leads (at this value of β) to 4-cyclical chaotic intervals Q'_4, then the homoclinic bifurcation of q_2 results in the pairwise merging of the intervals of Q'_4, giving rise to Q'_2, which

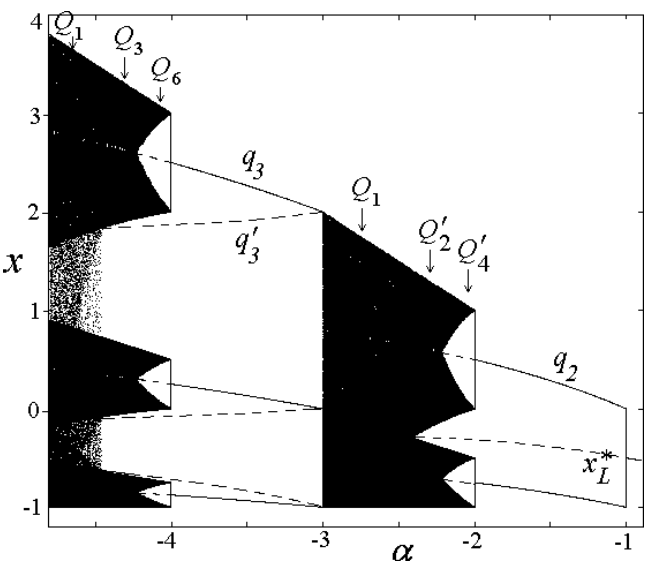

Fig. 2. 1D bifurcation diagram of the map f for $\beta = 0.5$, $\varepsilon = -1$ and $\alpha \in [-4.8, -0.95]$.

bifurcates to Q_1 due to the first homoclinic bifurcation of the fixed point x_L^* occurring when $f^3(0) = x_L^*$, at $\alpha = (-1 - \sqrt{1+4\beta})/2\beta|_{\beta=0.5} \approx -2.41$. At $\alpha = -(1+\beta)/\beta|_{\beta=0.5} = -3$ we have the "saddle-node" BCB (the lower boundary of $\Pi(q_3)$) giving rise to the attracting cycle q_3 and the repelling cycle q_3'. At $\alpha = -1/\beta^2|_{\beta=0.5} = -4$ the DFB of q_3 occurs, and there are three segments of periodic points: the segment $[0, f^3(0)]$ and its two images by f, that is $[f(0), f^4(0)]$ and $[f^5(0), f^2(0)]$. Each point of these segments (except for the points of q_3) is periodic of period 6. The DFB of q_3 gives rise to 6-cyclical chaotic intervals Q_6 which then bifurcates to Q_3 due to the homoclinic bifurcation of q_3 and, finally, the homoclinic bifurcation of q_3' leads to Q_1.

In general, at the parameter values related to the DFB of the attracting cycle q_k, that is for $(\alpha, \beta) : \alpha = -1/\beta^{(k-1)}$ (before the intersection point $(\alpha_k, \beta_k), \alpha < \alpha_k, \beta < \beta_k$), the map f has k segments each point of which (except for the points of q_k) is $2k$-periodic, or, if we consider the related map f^{2k}, it has k segments, each point of which is fixed.

To complete the description of the possible bifurcations occurring for the map f and, in particular, degenerate bifurcations of the fixed point x_L^* and the 2-cycle q_2, we note that the DFB of x_L^* taking place at $\alpha = -1$ for $\beta < -1$ is of subcritical type: Indeed, a repelling 2-cycle q_k' coexists with the attracting fixed point x_L^* before the bifurcation for $\alpha > -1, \beta < 1/\alpha$, so that at $\alpha = -1$ the cycle q_2' undergoes the BCB (its points -1 and 0 are the end points of the segment each point of which except x_L^* is 2-periodic), and after the bifurcation, that is for $\alpha < -1$, the cycle q_2' disappears, while x_L^* becomes repelling. Note also that the curve $\beta = 1/\alpha$ corresponds to the eigenvalue $\lambda = \alpha\beta = 1$ of the 2-cycle, and at such parameter values the points of the 2-cycle are located at infinity, that is the curve $\beta = 1/\alpha$ is related to the degenerate transcritical bifurcation (DTB) of the attracting cycle q_2 (for $\alpha < -1$) or of the repelling cycle q_2' (for $-1 < \alpha < 0$).

As it was mentioned in the Introduction the map f is used as normal form to study the BCB occurring in 1D PW smooth maps. In fact, the border-collision of the fixed point of f occurs at $\varepsilon = 0$ ($x_L^* = x_R^* = 0$), so varying ε through 0 (from $\varepsilon < 0$ to $\varepsilon > 0$ or vice versa) at some fixed values $(\alpha, \beta) = (\alpha^*, \beta^*)$ the dynamics of f changes due to this BCB (we exclude the trivial case $|\alpha| < 1, |\beta| < 1$ when crossing ε through 0 leads from the attracting fixed point on one side of the break point to the attracting fixed point on the other side). To see what kind of transition occurs in a nontrivial case, first recall that the (α, β)-bifurcation structures of the maps $f(x, \alpha, \beta, \varepsilon)$ and $f(x, \alpha, \beta, -\varepsilon)$ are symmetric with respect to $\alpha = \beta$, thus it is enough to consider in the (α, β)-bifurcation plane (see Fig. 1) the two points $(\alpha, \beta) = (\alpha^*, \beta^*)$ and $(\alpha, \beta) = (\beta^*, \alpha^*)$, and then the dynamics of f changes according to the dynamics related with these two points. For example, if we fix $(\alpha^*, \beta^*) = (-2, 0.8)$ then at $\varepsilon = 0$ the BCB leads from the attracting fixed point (corresponding to $(\alpha, \beta) = (0.8, -2)$ in Fig. 1) existing for $\varepsilon > 0$ to the attracting chaotic interval existing for $\varepsilon < 0$ (corresponding to $(\alpha, \beta) = (-2, 0.8)$ in Fig. 1).

All the possible BCB of the fixed point of f are summarized in Fig. 3, where it is also shown schematically the related 1D bifurcation diagrams for ε crossing 0 from a positive to negative value; the dashed region corresponds to the BCB from no attractor to cyclical chaotic intervals. Due to the fact that all the bifurcation curves for the map f have analytical expressions, all the BCB which can occur at $\varepsilon = 0$ are well classified. This allows to use the map f as the BCB normal form for 1D PW smooth maps (examples will be presented in the next subsections).

3.2. *1D linear — logistic map*

In this subsection we consider a PW smooth unimodal map g with one break point defined as

$$g : x \mapsto g(x) = \begin{cases} g_1(x) = rx, & 0 \le x \le \overline{x}; \\ g_2(x) = ax(1-x), & \overline{x} \le x \le 1; \end{cases} \qquad \overline{x} = 1 - \frac{r}{a}, \tag{8}$$

where a and r are real parameters: $a > 3$ and $0 < r < a$.

The dynamics of the map g were studied in detail in [Sushko *et al.*, 2005, 2006]. Here, we first discuss possible results of the degenerate bifurcation $\lambda = 1$ (DB1) occurring for the fixed point $x_L^* = 0$ at $r = 1$, whose effect is very similar to the DFB of the fixed point that we have seen in the previous example. Then we show without going into details how to apply the 1D BCB normal form (which is the skew-tent map f presented in the previous subsection) to classify the BCB of the attracting 2-cycle of the map g depending on the parameters.

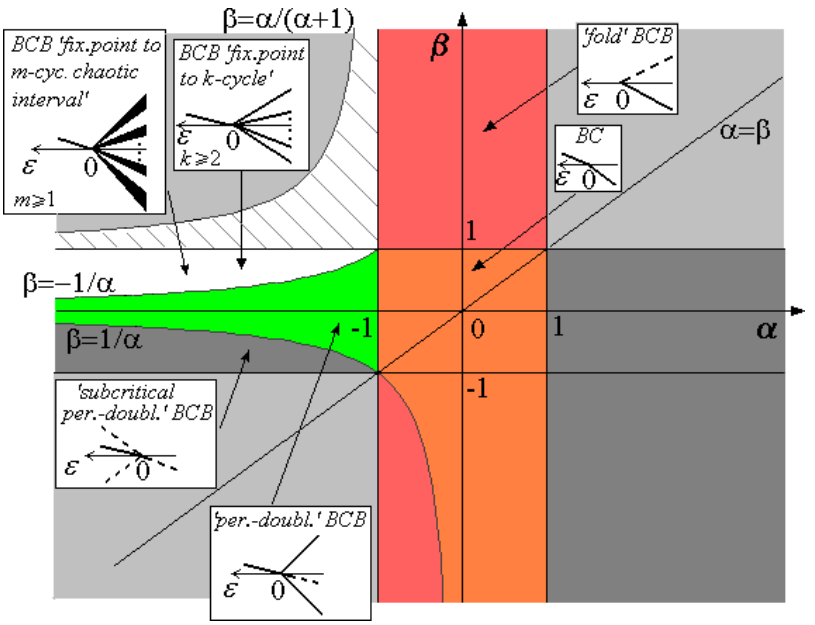

Fig. 3. Partition of the (α, β)-parameter plane into the regions of qualitatively similar dynamics of the map f (see also Fig. 1); The related BCB of the fixed point of f occurring at $\varepsilon = 0$ are illustrated schematically by 1D bifurcation diagrams.

The fixed point x^*_L is globally attracting for $r < 1$. At $r = 1$ there is a segment $(-\infty, \overline{x}]$ each point of which is fixed. To see the result of the DB1, that is, to see what kind of attractor appears after this bifurcation, first note that the interval $I = [0, 1]$ is trapping for the map g if $(r, a) \in D$, where

$$D = \left\{(r, a) : 1 < r < 2, a \le \frac{r^2}{r-1}\right\} \cup \{(r, a) : r \ge 2, a \le 4\}.$$

Note also that for $r > 1, 1 < a < 3$ the second fixed point $x^*_R = 1 - 1/a$ is attracting for any $x \in I$. In [Sushko *et al.*, 2005, 2006] the bifurcation structure of the (r, a)-parameter plane of the map g was described in detail, showing that for $(r, a) \in D$ the map g can have attracting cycles γ_n of any period k, as well as k-cyclical chaotic intervals G_k of any period k.

Figure 4 shows a part of the 2D bifurcation diagram of the map g in the (r, a)-parameter plane in which the stability region of the fixed point x^*_L (shown in orange) is bounded by the curve $r = 1$ of the degenerate bifurcation DB1. The stability region of the attracting 2-cycle γ_2 of period 2 (shown in green) is bounded by the BCB curve denoted $\mathcal{B}_2$ (whose analytic equation is given below); $\mathcal{H}_{2^k}$, for any $k \ge 1$, denotes the curve of first homoclinic bifurcation of the repelling cycle of period 2^k; $\mathcal{H}_1$ is the curve of first homoclinic bifurcation of the fixed point x^*_R, given by $f^3(\overline{x}) = x^*_R$.

For parameter values belonging to the region bounded by the curves $\mathcal{H}_{2^k}$ and $\mathcal{H}_{2^{k+1}}$ the related attractor of the map g consists in 2^{k+1}-cyclical chaotic intervals $G_{2^{k+1}}$, and for parameter values taken above the curve $\mathcal{H}_1$ the map g has a one-piece attracting chaotic interval G_1. It is possible to see that the homoclinic curves intersect the curve of the DB1 given by $r = 1$ so that, depending on the value of the parameter a, this bifurcation can lead to cyclical chaotic intervals G_{2^k} of any integer $k \ge 0$.

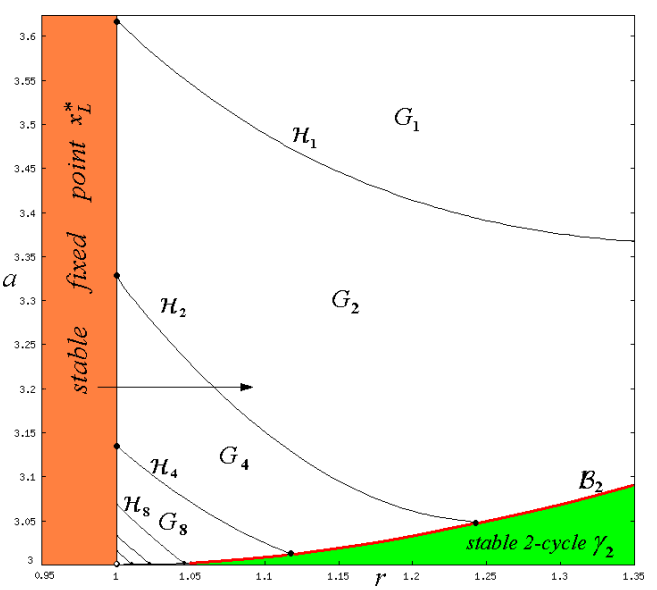

Fig. 4. A portion of the 2D bifurcation diagram of the map g in the (r, a)-parameter plane.

Thus, for example, for $a > 3.618$ the DB1 of the fixed point x_L^* gives rise to the attracting chaotic interval G_1. Note that the point $(r, a) = (1, 3)$ of the (r, a)-parameter plane in particular: It is an accumulation point for the curves $\mathcal{H}_{2^k}$ as $k \to \infty$, so that if the parameter point moves transversely through all the curves $\mathcal{H}_{2^k}$, approaching the point $(r, a) = (1, 3)$, then we have an infinite cascade of period-doubling bifurcations for the cyclical chaotic intervals $G_2 \Rightarrow G_{2^2} \Rightarrow G_{2^3} \Rightarrow \cdots$, the size of which reduces to 0. So, the DB1 of the fixed point x_L^* can give rise to cyclical chaotic intervals G_{2^k}, where $k \to \infty$ as $a \to 3$.

Figure 5 presents a 1D bifurcation diagram for parameter values $a = 3.2$ and $r \in [0.99, 1.1]$ (see the straight line with an arrow in Fig. 4), at which it is possible to observe the following bifurcation sequence: $x_L^* \Rightarrow G_{2^2} \Rightarrow G_2$.

Let us now show how the 1D BCB normal form f given in (1) can be used to study the possible kinds of BCB of the cycle γ_n of the map g (for the details see [Sushko *et al.*, 2006]). Let $\mathcal{B}_n$ denote a curve in the (r, a)-parameter plane related to the BCB of γ_n. It is given by $\mathcal{B}_n = \{(r, a) : g^n(\overline{x}) = \overline{x}\}$ (see, for example, Fig. 4 in which a part of the curve $\mathcal{B}_2$ is shown; $\mathcal{B}_2$ is given by $a = 1/r + 1 + r, 1 < r < r_0$, where $r_0 = (\sqrt{6} + \sqrt{2})/2$). Let the (r, a)-parameter point cross $\mathcal{B}_n$ transversely at some point $(r^*, a^*) \in \mathcal{B}_n$ in such a way that γ_n is attracting before the collision. The result of this collision depends on the left and right side derivatives of g^n at $x = \overline{x}, (r, a) = (r^*, a^*)$, denoted α and β, respectively:

$$\alpha = \lim_{x \to \overline{x}_-} \frac{d}{dx} g^n(x); \quad \beta = \lim_{x \to \overline{x}_+} \frac{d}{dx} g^n(x). \quad (9)$$

Namely, if we consider the map f given in (1) with such parameters α and β and let the parameter ε vary through 0, then the BCB of the fixed point of the PW linear map f and the BCB of the fixed point of the PW smooth map g^n are of the same kind, that is, the border collision occurring for the cycle γ_n of the map g at $(r, a) = (r^*, a^*) \in \mathcal{B}_n$, is of the same kind as the border collision of the fixed point of the map f occurring at $\varepsilon = 0$.

Coming back to our example: The BCB curve $\mathcal{B}_2$ of the cycle γ_2 of the map g in (8) in terms of the related parameters α and β is given by $\beta = -4\alpha(\sqrt{5 - 4\alpha} + \alpha - 1)/(\sqrt{5 - 4\alpha} - 1)^2, |\beta| < 1$, and it is the curve denoted $\mathcal{L}_2$ in Fig. 6. Let $\mathcal{L}_2^*$ denote the curve symmetric with respect to $\alpha = \beta$. This curve is located in the range $|\alpha| < 1$ corresponding to the attracting fixed point of the map f (see Fig. 1), so, it is related to the attracting fixed point of g^2 (or, in other words, to the attracting cycle γ_2 of g before the border-collision). Now it is possible to see which bifurcation curves the curve $\mathcal{L}_2$ intersects and we can deduce which attractors of g appear due to the BCB of γ_2 (note that the period of such attractors of g is doubled with respect to those indicated in Fig. 6, as the curve $\mathcal{L}_2$ is related to the BCB of the fixed point of g^2). Given that in Fig. 4 only a part of the curve $\mathcal{B}_2$ is shown (the related part of the curve $\mathcal{L}_2$ is the one shown in red for $\alpha \in [-2.17, -1]$), only the BCBs $\gamma_2 \Rightarrow G_{2^k}, k \geq 1$, are observable in Fig. 4.

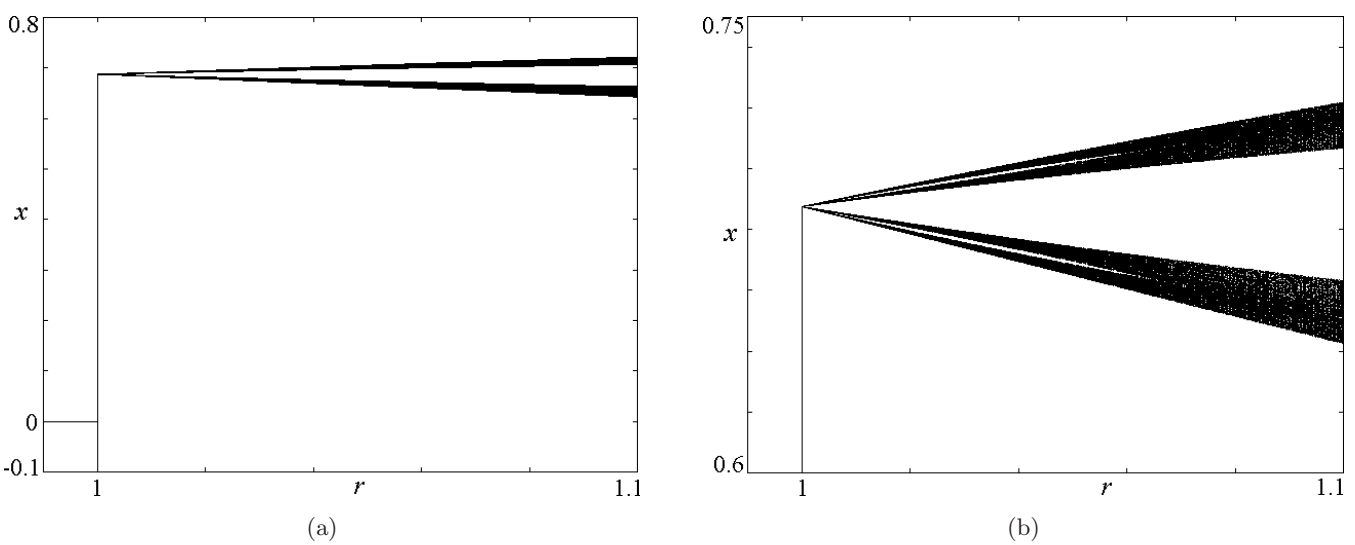

Fig. 5. (a) 1D bifurcation diagram of the map g at $a = 3.2$, $r \in [0.99, 1.1]$, and (b) its enlargement.

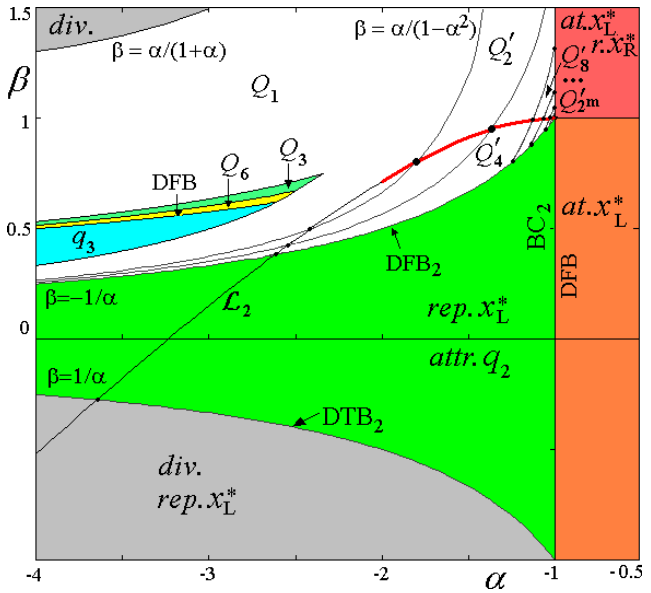

Fig. 6. An enlarged part of the 2D bifurcation diagram of the skew-tent map f in the (α, β)-parameter plane shown in Fig. 1: Here $\alpha \in [-4, -0.5]$ and $\beta \in [0, 1.5]$; The curve $\mathcal{L}_2$ is related to the BCB of the attracting fixed point of the map g^2 where g is given in (8).

In particular, the parameter point $(r, a) = (1, 3)$ corresponding to $(\alpha, \beta) = (-1, 1)$, is an accumulation point not only for the degenerate bifurcations DB1 $x_L^* \Rightarrow G_{2^k}$ (at $r = 1$ and $k \to \infty$ as $a \to 3$), but also for the BCB $\gamma_2 \Rightarrow G_{2^k}$, where $k \to \infty$ as $r \to 1$ and $a = (1/r + 1 + r) \to 3$.

3.3. *1D power — linear-fractional map*

Consider now one more example: A 1D PW smooth map ϕ which is defined as follows:

$$\phi : x \mapsto \phi(x) = \begin{cases} f(x) = rx^{1-\frac{1}{\sigma}}, & 0 < x \le 1 \\ g(x) = \dfrac{rx}{1+\theta(x-1)}, & x \ge 1 \end{cases} \tag{10}$$

where $\theta = (1 - (1/\sigma))^{1-\sigma}, \sigma > 1, r > 0$. The map ϕ is studied in [Gardini *et al.*, 2008].

The function $f(x)$ is monotonic increasing as $f'(x) = r(1 - (1/\sigma))x^{-\frac{1}{\sigma}} > 0$. It has a unique fixed point $x_L^* = r^\sigma$ which exists (in its region of definition: $x < 1$) as long as $r < 1$, and when it exists, it is always stable, as $0 < f'(x_L^*) = (1 - (1/\sigma)) < 1$. Furthermore, it is globally attracting except for the origin. At $r = 1$ a BCB occurs: $x_L^* = 1$, which we shall comment here below, and can lead to an attracting 2-cycle, as well as to attracting cyclical chaotic intervals Q_m, where $m = 1, 2, 4$.

Let us first consider the DFB which can occur in the map ϕ. The function $g(x)$ is monotonic decreasing and convex (as $g'(x) = -(r(\theta-1)/(1+\theta(x-1))^2) < 0$, and $g''(x) > 0$) and it has a unique fixed point $x_R^* = 1+((r-1)/\theta)$ which exists for any $r > 1$ (at $r = 1$ it undergoes a BCB: $x_R^* = 1$), but it may be stable or unstable. From $g'(x_R^*) = -(\theta - 1)/r$ we have that it is locally stable for $r > (\theta - 1)$, and it is easy to see that it is also globally attracting. The interesting regime is the interval $1 < r < (\theta - 1)$, and as r varies in this interval the dynamics depend on the value of the other parameter σ. At the bifurcation value $r = (\theta-1)$ a DFB occurs: all the points of the segments $[1, x_R^*)$ and $(x_R^*, 1]$ are periodic of period 2. We can show this by using the change of variable which puts x_R^* in the origin. That is, let $y = x - x_R^*$ then

$$h(y) = g(y + x_R^*) - x_R^* = \frac{(1-\theta)y}{\theta y + r}$$

and

$$h^2(y) = \frac{(1-\theta)^2 y}{y(\theta(1-\theta) + r\theta) + r^2}$$

so that at the bifurcation value $r = (\theta - 1)$ we have $h^2(y) = y$, and $\phi([g(r), r]) = [g(r), r]$. In Fig. 7(a) we show the map ϕ (whose graph is in green) at the DFB of the fixed point, when $\phi^2(x) = x$ in the interval $[g(r), r]$, leading to a unique attracting 2-cycle, with periodic points on opposite side with respect to $x = 1$.

In Fig. 7(b) we show the DFB of the 2-cycle, occurring when $\phi^4(1) = g \circ f \circ g^2(1) = 1$, at which we have $\phi^4(x) = x$ in two intervals: $[\phi^3(r), r]$ and $[g(r), \phi^4(r)]$, leading to 4-cyclical chaotic intervals Q_4. The rigorous proof of all the bifurcations occurring in the map ϕ are not easy because of the complex analytical expressions. However, a numerical proof is summarized in Fig. 8(a), where we present a 2D bifurcation diagram in the (r, σ)-parameter plane in which different colors correspond to different dynamic regimes of the map ϕ. For any fixed value of σ, $\sigma > 2$, as r decreases from a value larger than $(\theta - 1)$, the transition is always of the same type: the DFB of the fixed point is followed by the DFB of the 2-cycle occurring at a value $r = r_4(\sigma)$ (at which the condition $\phi^4(1) = g \circ f \circ g^2(1) = 1$ is fulfilled), leading to 4-cyclical chaotic intervals Q_4. The next bifurcation gives rise to 2-cyclical chaotic intervals Q_2 due to the first homoclinic bifurcation of the 2-cycle when the point $x = r$ is preperiodic to this cycle, occurring at a value $r = r_2(\sigma)$, at which

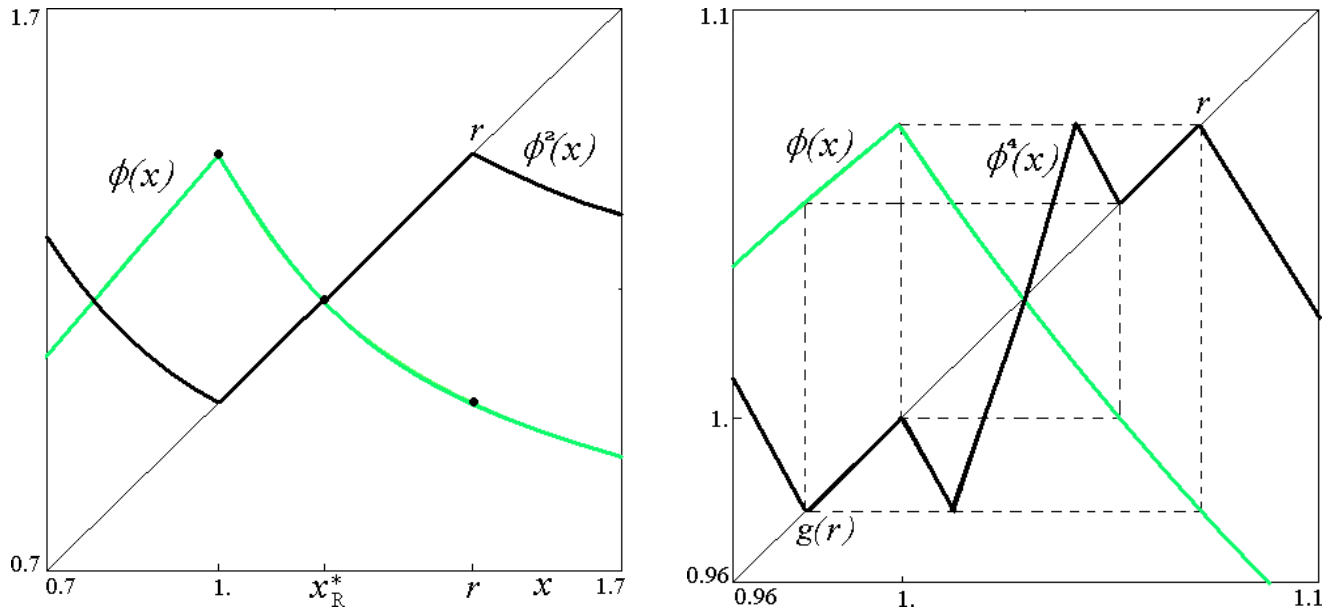

Fig. 7. (a) The map ϕ (whose graph is in green) at the DFB of the fixed point at $r = (\theta - 1) = 1.441408, \sigma = 5$; (b) the DFB of the 2-cycle at $r = 1.0725, \sigma = 5$.

the condition $\phi^5(1) = g^2 \circ f \circ g^2(1) = x_R$ is fulfilled, where $x_R > 1$ denotes the periodic point of the 2-cycle in the right side. Then the two chaotic intervals of Q_2 may merge into a one-piece chaotic interval Q_1 due to the first homoclinic bifurcation of the fixed point x^*_R, when the point $x = r$ is preperiodic to it, occurring at a value $r = r_1(\sigma)$ at which the condition $\phi^3(1) = f \circ g^2(1) = x^*_R$ is fulfilled, that is when

$$r\left(\frac{r^2}{1+\theta(r-1)}\right)^{(1-\frac{1}{\sigma})} = 1 + \frac{r-1}{\theta}. \qquad (11)$$

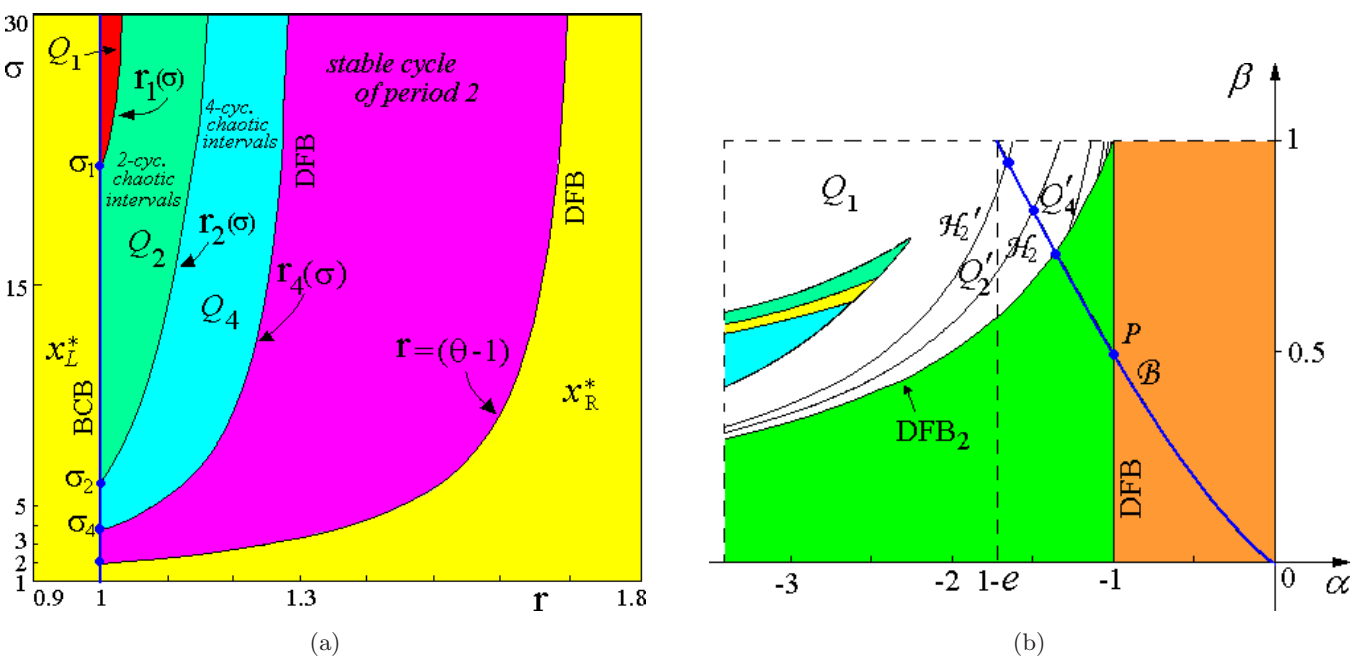

Fig. 8. In (a) 2D bifurcation diagram in the (r, σ)-parameter plane. The yellow color corresponds to a stable fixed point in the map ϕ followed by a region of attracting 2-cycle q_2, and in sequence the colored regions correspond to k-cyclical chaotic intervals Q_k, for $k = 4, 2, 1$ respectively. In (b) the BCB curve $\mathcal{B}$ in the (α, β) parameter plane.

To rigorously prove which kind of BCB occurs at $r = 1$ we make use of the BCB normal form f given in (1) and described in Sec. 3.1. The result of the BCB of the fixed point depends on the left and right side derivatives of $\phi(x)$ evaluated at $x = 1$ for $r = 1 : \alpha = \lim_{x\to 1_-}(d/dx)\phi(x)$ and $\beta = \lim_{x\to 1_+}(d/dx)\phi(x)$, that is:

$$\alpha = \left(1 - \frac{1}{\sigma}\right) \in (0, 1), \quad \beta = (1 - \theta) < 0. \tag{12}$$

Substituting first $\theta = (1 - (1/\sigma))^{1-\sigma}$ and then $\sigma = 1/(1 - \alpha)$ into (12) we get the expression of the BCB curve of the fixed point $x^* = 1$ in terms of the parameters α and β, which is denoted as $\mathcal{B}^*$,

$$\mathcal{B}^* : \beta = 1 - \alpha^{\alpha/(\alpha-1)}. \tag{13}$$

Its symmetric one is denoted as $\mathcal{B}$:

$$\mathcal{B} : \alpha = 1 - \beta^{\beta/(\beta-1)}$$

and it is plotted in blue in Fig. 8(b).

The curve $\mathcal{B}$ in Fig. 8(b) corresponds to the vertical line $r = 1$ in the bifurcation diagram in Fig. 8(a). We can see that $\mathcal{B}$ intersects the straight line $\alpha = -1$ at a point P which is $(\alpha, \beta) = (-1, 0.5)$, related to the DFB of the fixed point at $(r, \sigma) = (1, 2)$ in Fig. 8(a), the intersection with the DFB of the 2-cycle corresponds to the point σ_4 in Fig. 8(a), and the intersections with the homoclinic bifurcation curves $\mathcal{H}_2$, and $\mathcal{H}'_2$ in Fig. 8(b) correspond to the points σ_2 and σ_1, respectively, in Fig. 8(a).

4. Degenerate Bifurcations in the 2D BCB Normal Form

To give examples of the degenerate bifurcations in 2D PW smooth maps we use the 2D BCB normal form $F : \mathbb{R}^2 \to \mathbb{R}^2$ proposed in [Nusse & Yorke, 1992], which is nowadays quite intensively studied by many researchers in order to classify possible BCB in 2D PW smooth maps (see, e.g. [Banerjee & Grebogi, 1999; Zhusubaliyev *et al.*, 2006; Sushko & Gardini, 2008; Simpson & Meiss, 2008; Gardini *et al.*, 2009a], etc.). The map F is given by two linear maps F_L and F_R which are defined in two half planes L and R:

$$F : (x, y) \mapsto \begin{cases} F_L(x, y), & (x, y) \in L; \\ F_R(x, y), & (x, y) \in R; \end{cases} \tag{14}$$

where

$$F_L : \begin{pmatrix} x \\ y \end{pmatrix} \mapsto \begin{pmatrix} \tau_L x + y + \mu \\ -\delta_L x \end{pmatrix}, \quad L = \{(x, y) : x \le 0\}; \tag{15}$$

$$F_R : \begin{pmatrix} x \\ y \end{pmatrix} \mapsto \begin{pmatrix} \tau_R x + y + \mu \\ -\delta_R x \end{pmatrix}, \quad R = \{(x, y) : x > 0\}. \tag{16}$$

Here τ_L, τ_R are the traces and δ_L, δ_R are the determinants of the Jacobian matrix of the map F in the left and right halfplanes, i.e. in L and R, respectively, $\mathbb{R}^2 = L \cup R$.

By using the change of variables $(u = x/|\mu|, v = y/|\mu|)$, and then changing (u, v) into (x, y), we are lead to the map as in (15) and (16) with $\mu = -1$ or $\mu = 1$. However, in order to determine all the possible bifurcations it is enough to consider only one of the two cases, say $\mu = +1$, as the bifurcations associated with the second case $\mu = -1$ can be obtained using a symmetry property. In fact, with the change of variables $(u = -x, v = -y)$ the two cases are topologically conjugate, i.e. there is a symmetry in the $(\tau_L, \tau_R, \delta_L, \delta_R)$-parameter space with respect to the surfaces $\tau_L = \tau_R$ and $\delta_L = \delta_R$. So, it is enough to describe the bifurcations of F at $\mu = 1$ (which is the same for any $\mu > 0$), then for $\mu = -1$ (which is the same for any $\mu < 0$) we have similar results exchanging the index L into R and vice versa.

Let L^* and R^* denote the fixed points of F_L and F_R determined, respectively, by

$$\left(\frac{\mu}{1 - \tau_i + \delta_i}, \frac{-\delta_i \mu}{1 - \tau_i + \delta_i}\right), \quad i = L, R.$$

L^* is the fixed point of the map F if $\mu/(1-\tau_L+\delta_L) \le 0$, otherwise it is a so-called virtual fixed point which we denote by $\overline{L}^*$. Similarly, R^* is the fixed point of F if $\mu/(1 - \tau_R + \delta_R) \ge 0$, otherwise it is a virtual fixed point denoted by $\overline{R}^*$. If the parameter μ varies through 0, the fixed points (actual or/and virtual) cross the border line $x = 0$, so that the collision with it occurs at the value $\mu = 0$, at which L^* and R^* merge with the origin $(0, 0)$.

The border line $x = 0$ denoted LC_{-1}, as well as its backward and forward images by F are called *critical lines* [Mira *et al.*, 1996]. The first image of LC_{-1} is the straight line $LC = F(LC_{-1}) = \{(x, y) : y = 0\}$, while $LC_i = F^i(LC), i > 0$, called critical line of rank i, is in general a broken line.

The stability of the fixed point R^* is defined by the eigenvalues $\lambda_{1,2(R)}$ of the Jacobian matrix of the

map F_R, which are

$$\lambda_{1,2(R)} = \frac{(\tau_R \pm \sqrt{\tau_R^2 - 4\delta_R})}{2}. \quad (17)$$

The triangle of stability of R^*, say $S(R^*)$, is defined as follows:

$$S(R^*) = \{(\delta_R, \tau_R) : 1 + \tau_R + \delta_R > 0, \\ 1 - \tau_R + \delta_R > 0, 1 - \delta_R > 0\}. \quad (18)$$

The eigenvalues $\lambda_{1,2(L)}$ of the Jacobian matrix of F_L and the triangle of stability $S(L^*)$ are defined as in (17) and (18), respectively, putting the index L instead of R.

In the next subsections we present examples of the degenerate flip bifurcation, as well as super- and subcritical center bifurcation of the fixed point R^*, and also degenerate bifurcations of the cycle of period 3.

4.1. *Degenerate flip bifurcation of the fixed point R**

So, let $\mu = 1, (\delta_L, \tau_L) \in S(L^*), (\delta_R, \tau_R) \in S(R^*)$, so that the map F has the attracting fixed point R^* and the virtual attracting fixed point $\overline{L}^*$ (it is clear that even if the second fixed point is virtual, its stability defines dynamics in L). In this section, we describe the DFB of R^* occurring when the (δ_R, τ_R)-parameter point leaves the triangle of stability $S(R^*)$ crossing the boundary $1 + \tau_R + \delta_R = 0$ which corresponds to $\lambda_{2(R)} = -1$.

First note that in [Maistrenko *et al.*, 1998] a 2D PW linear map was considered, the fixed point of which undergoes the DFB (to indicate this bifurcation the authors have used the term "flip bifurcation"). It was shown numerically that depending on the parameters this bifurcation can lead to an attracting cycle of period 2, or to a cyclical chaotic attractor of period 2^k, where $k \geq 1$ can be any integer. In the present section, we show (without going into details) that an analogous transition can be observed due to the DFB of the fixed point R^* of the map F.

Let the eigenvalues $\lambda_{1,2(R)}$ be real and W_l^s (respectively W_l^u) denote a local invariant set of R^* related to the eigenvalue $\lambda_{1(R)}$ (respectively $\lambda_{2(R)}$). It is easy to show that at $1 + \tau_R + \delta_R = 0$ corresponding to the DFB of R^* we have $W_l^u = [A, B], A = (0, \lambda_{1(R)}/(1 - \lambda_{1(R)})) \in LC_{-1}, B = (1/(1 - \lambda_{1(R)}), 0) \in LC$; Each point of $[A, B]$ except R^* is periodic of period 2. If the (δ_R, τ_R)-parameter point crosses the DFB line the fixed point R^* becomes a saddle.

To see the result of this bifurcation we first obtain stability conditions for an attracting cycle of period 2 denoted γ_2, which, obviously, has one point in R and one in L. Let $\lambda_{1,2(\gamma_2)}$ be the eigenvalues of the Jacobian matrix of the map $F^2 = F_R \circ F_L$. The region $S(\gamma_2)$ of existence and stability of γ_2 can be bounded by at most four straight lines: The first one denoted BCB_2 corresponds to the BCB of γ_2 and three others are related to the degenerate bifurcations, namely, to the DTB ($\lambda_{1(\gamma_2)} = 1$), DFB ($\lambda_{2(\gamma_2)} = -1$) and the center bifurcation denoted CB_2 ($|\lambda_{1,2(\gamma_2)}| = 1$):

$$\tau_R = -1 - \delta_R; \quad \mathrm{BCB}_2$$

$$\begin{cases} \tau_R = \dfrac{(1 + \delta_R)(1 + \delta_L)}{\tau_L}, & \tau_L \neq 0 \\ \delta_R = 1, & \tau_L = 0 \end{cases}; \quad \mathrm{DTB}_2$$

$$\begin{cases} \tau_R = \dfrac{(\delta_R - 1)(1 - \delta_L)}{\tau_L}, & \tau_L \neq 0 \\ \delta_R = -1, & \tau_L = 0 \end{cases}; \quad \mathrm{DFB}_2$$

$$\delta_R = \frac{1}{\delta_L}, \delta_L \neq 0. \quad \mathrm{CB}_2$$

In the (δ_R, τ_R)-parameter plane all the four straight lines, or only three of them, bound the region $S(\gamma_2)$ depending on τ_L and δ_L. Moreover, this region can also be unbounded (when the straight lines DTB_2 and DFB_2 are parallel, that holds for $\delta_L = 0, \tau_L \neq 0$, or for $\tau_L = 0$). Figure 9 presents $S(R^*)$ and $S(\gamma_2)$ at $\tau_L = -0.1, \delta_L = 0.5$.

One can immediately note that the equations for the DFB boundary of $S(R^*)$ and the BCB boundary of $S(\gamma_2)$ are the same, so that the DFB of the fixed point R^* can lead to the attracting cycle γ_2. Following some simple geometrical reasoning it can be easily shown that for $\tau_L < 0$ the DFB of R^* always leads to the attracting cycle γ_2 (as it occurs in the case presented in Fig. 9): Indeed for $\tau_L < 0$ at the intersection point of DFB_2 and BCB_2 we have $\delta_R > 1$, so that if the (δ_R, τ_R)-parameter point crosses the DFB boundary of $S(R^*)$ the fixed point R^* can bifurcate only to the attracting cycle γ_2.

For $\tau_L > 0$ the DFB of R^* can lead not only to the attracting 2-cycle, but to a cyclical chaotic attractor as well. To see this first note that for $\delta_L = 0, \delta_R = 0$ the dynamics of F are reduced to the critical line LC on which it is defined as the skew-tent map f given in (1), where $\alpha = \tau_L > 0$,

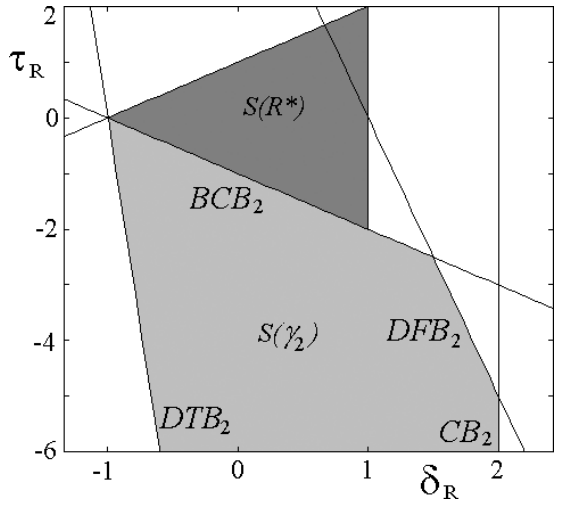

Fig. 9. The regions $S(R^*)$ and $S(\gamma_2)$ at $\tau_L = -0.1$, $\delta_L = 0.5$.

$\beta = \tau_R < 0, \mu > 0$. For such a map the point $(\tau_L, \tau_R) = (1, -1)$ is particular (see Sec. 3.1) being an accumulation point for the curves related to a cascade of the period-doubling bifurcations of the cyclical chaotic intervals $Q_{2^k} \Rightarrow Q_{2^{k+1}}$, where $k \to \infty$ as $(\tau_L, \tau_R) \to (1, -1)$. It is natural to suppose that if the intersection point of DFB_2 and BCB_2 is $(\delta_R, \tau_R) = (0, -1)$, that holds for $\tau_L = 1 - \delta_L$, then this point is also an accumulation point for the curves corresponding to infinite period-doubling cascade of cyclical chaotic attractors of the map F.

So, let $\tau_L = 1 - \delta_L$. Recall that we consider $(\delta_L, \tau_L) \in S(L^*)$, so that if $\tau_L = 1 - \delta_L$, then it follows that $\delta_L > 0$ (Fig. 11 shows the regions $S(R^*)$ and $S(\gamma_2)$ at $\delta_L = 0.4, \tau_L = 1 - \delta_L = 0.6$). Then, varying the value of δ_R through 0 at fixed $\delta_L > 0$, the map F changes its invertibility, being invertible for $\delta_R > 0$ and noninvertible (of $Z_0 - Z_2$ type) for $\delta_R < 0$. At $\delta_R = 0$ we have $\lambda_{1(R)} = 0$, so that the whole region R is mapped into the critical line LC (the map F in such a case is noninvertible of $Z_0 - Z_\infty - Z_1$ type). It can be easily shown that the dynamics of F are reduced to a one-dimensional subset of the phase space, namely, to a tree made up of a finite number of images of LC. The structure of such a tree, the attractors on it and their bifurcations are described in detail for an analogous 2D PW linear map in [Sushko *et al.*, 1999]. In particular, it is proved that one can observe a cascade of the period-doubling bifurcations of the cyclical chaotic attractors located on the tree. Let G_m denote a cyclical chaotic attractor of period m of the map F. Figure 10 shows two examples of the tree made up by three halflines with two attractors on it: An attracting 3-cycle (whose basin of attraction is bounded by the stable set of the related saddle 3-cycle) coexists with a one-piece chaotic attractor G_1 (Fig. 10(a), $\tau_L = 0.6, \delta_L = 0.4, \delta_R = 0, \tau_R = -2$, point a in Fig. 12), or with a two-piece chaotic attractor G_2 (Fig. 10(b), $\tau_R = -1.7$, point b in Fig. 12). Increasing the value of τ_R, we observe the cascade of period-doubling bifurcations of the cyclical chaotic attractors $G_{2^k} \Rightarrow G_{2^{k+1}}, k = 0, 1, \ldots,$ where $k \to \infty$ as $\tau_R \to -1$ (see Figs. 11 and 12). Thus, for example, the transition $G_1 \Rightarrow G_2$ occurs at $\tau_R \approx -1.77$ due to the homoclinic bifurcation of R^*. With further increasing of τ_R the homoclinic bifurcation of γ_2 leads to G_4, then the homoclinic bifurcation of a 4-cycle results in G_8, and so on.

Let now $\tau_L = 1 - \delta_L, \delta_R \neq 0$. In Fig. 11, we show a part of the (δ_R, τ_R)-parameter plane at $\tau_L = 0.6, \delta_L = 0.4$ in which the regions $S(R^*), S(\gamma_2)$ and $S(\gamma_3)$ are plotted (the equations for the boundaries of $S(\gamma_3)$ are given in (22)–(25)). The rectangle in Fig. 11 is presented enlarged in Fig. 12 where also shown are the numerically obtained curves related to the following homoclinic bifurcations: The curve H_3 is related to the first homoclinic bifurcation of the saddle 3-cycle giving rise to the contact of the chaotic attractor G_1 with its basin boundary (formed by the stable set of the saddle 3-cycle); The curve H_1 separating the regions of G_2 and G_1 is related to the first homoclinic bifurcation of R^*; the curves separating the regions of $G_{2^{k+1}}$ and $G_{2^k}, k \geq 1$, correspond to the first homoclinic bifurcation of the 2^k-cycle. The parameter point $(\delta_R, \tau_R) = (0, -1)$ is the accumulation point for such homoclinic curves: on the right lower corner of Fig. 12 an enlargement of the window indicated by the dashed line is shown in which the regions of 2^k-cyclical chaotic attractors G_{2^k} can be clearly seen for $k = 3, 4, 5$.

Thus Fig. 12 demonstrates that the DFB of the fixed point R^* can lead to the 2^k-cyclical chaotic attractor G_{2^k} for any $k \geq 1$, as well as the DFB of the attracting 2-cycle γ_2 can lead to the 2^k-cyclical chaotic attractor G_{2^k} for any $k \geq 2$.

4.2. *Super- and subcritical center bifurcation of the fixed point*

In this subsection we give examples of the super- and subcritical center bifurcations of R^*. The *supercritical* center bifurcation of the fixed point R^* occurring at $\delta_R = 1, \tau_R \in (-2, 2)$, is described in

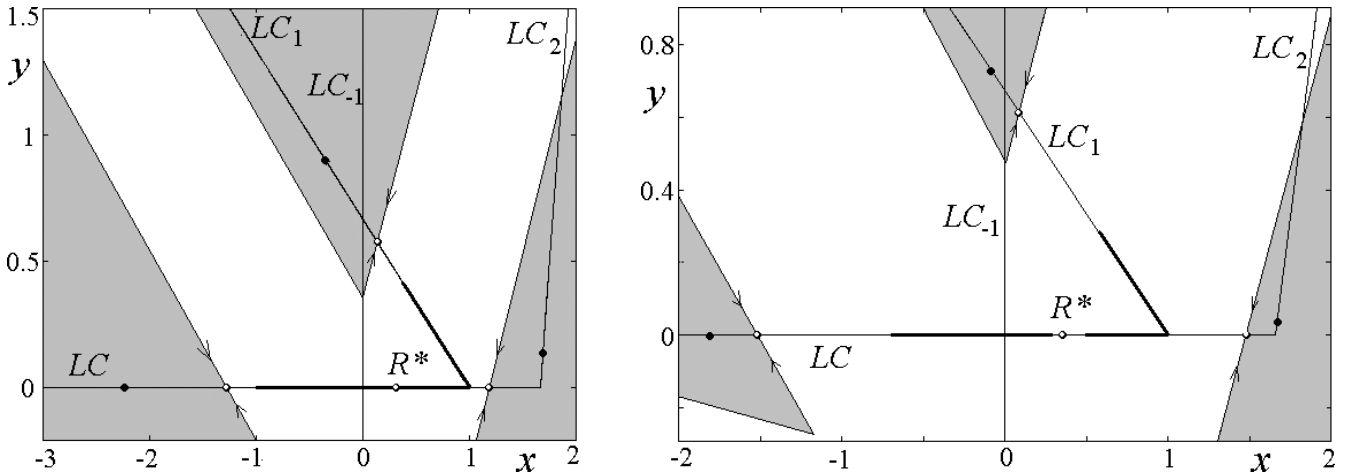

Fig. 10. Attracting 3-cycle (its basin of attraction is shown in grey) coexisting with (a) a one-piece chaotic attractor of F at $\tau_L = 0.6, \delta_L = 0.4, \delta_R = 0, \tau_R = -2$;.(b) two-piece chaotic attractor at $\tau_R = -1.7$.

detail in [Sushko & Gardini, 2008] (see also [Simpson & Meiss, 2008]) in the case in which the virtual fixed point $\overline{L}^*$ is attracting, that is for $(\tau_L, \delta_L) \in S(L^*)$. Below we recall some results and give an example of an attracting invariant closed curve born due to such a bifurcation. Then we present a new result related to the *subcritical* center bifurcation of R^* occurring at $\delta_R = 1, (\tau_L, \delta_L) \notin S(L^*)$.

At the parameter values $\delta_R = 1, \tau_R \in (-2, 2)$ (independently on τ_L and δ_L) related to the center bifurcation of R^*, there are two possibilities:

- *if F_R is defined by a rotation matrix with an irrational rotation number ρ, which holds for $\delta_R = 1$, and*

$$\tau_R = \tau_{R,\rho} \stackrel{\text{def}}{=} 2\cos(2\pi\rho), \tag{19}$$

then in the phase space of the map F there exists an invariant region Q, bounded by the invariant ellipse E given by

$$x^2 + y^2 + \tau_{R,\rho} xy - x + y = -\frac{1}{4}, \tag{20}$$

such that any initial point $(x_0, y_0) \in Q \backslash R^*$ belongs to a quasiperiodic orbit dense in the corresponding invariant ellipse of F_R;

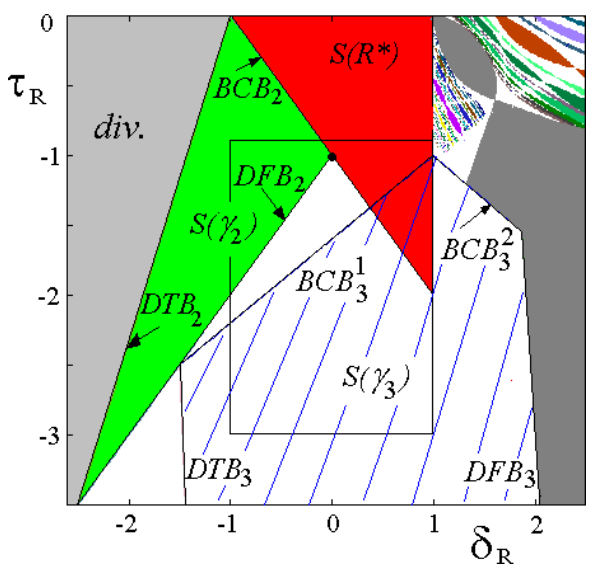

Fig. 11. The regions $S(R^*), S(\gamma_2)$ and $S(\gamma_3)$ in the (δ_R, τ_R)-parameter plane at $\tau_L = 0.6, \delta_L = 0.4$.

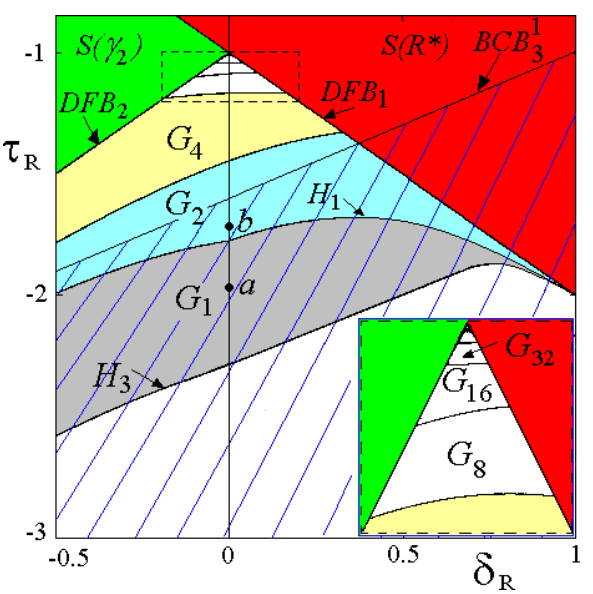

Fig. 12. Enlargement of the window indicated in Fig. 11, with the regions corresponding to 2^k-cyclical chaotic attractors $G_{2^k}, k \geq 0$. The window indicated by the dashed line is enlarged in the right lower corner.

- *if F_R is defined by a rotation matrix with a rational rotation number m/n, which holds for $\delta_R = 1$, and*

$$\tau_R = \tau_{R,m/n} \stackrel{\text{def}}{=} 2\cos\left(\frac{2\pi m}{n}\right), \qquad (21)$$

then in the phase space of the map F there exists an invariant polygon $P_{m/n}$ with n edges whose boundary is made up by the generating segment $S_{-1} \subset LC_{-1}$ and its $n-1$ images $S_i = F_R(S_{i-1}) \subset LC_i$, $i = 0, \ldots, n-2$. Any initial point $(x_0, y_0) \in P \backslash R^*$ is n-periodic with rotation number m/n.

(Note that in the case $m = 1$ the end points of the generating segment S_{-1} are $(0, -1)$ and $(0, 0)$; in [Sushko & Gardini, 2008] it has been explained how to obtain S_{-1} for $m \neq 1$.)

It can be shown that if $(\tau_L, \delta_L) \in S(L^*)$ then the invariant region ($P_{m/n}$ or Q) is attracting. In such a case after the center bifurcation, that is for $\delta_R = 1 + \varepsilon$ at some sufficiently small $\varepsilon > 0$, the boundary of the former invariant region is transformed into an *attracting closed invariant curve* $\mathcal{C}$ on which the map F is reduced to a rotation, so that we have a piecewise linear analogue of the *supercritical* Neimark–Sacker bifurcation. Indeed, similar to the Neimark–Sacker bifurcation occurring for smooth maps, at a rational rotation m/n two cycles of period n are born at the center bifurcation, one attracting and one saddle, and the closure of the unstable set of the saddle cycle approaching points of the attracting cycle forms the curve $\mathcal{C}$. Differently from the smooth case such a curve appears not in a neighborhood of the fixed point: Obviously, its position is defined by the distance of the fixed point from the critical line LC_{-1}. Moreover, the curve $\mathcal{C}$ is not smooth, but a piecewise linear set, which in general has infinitely many corner points accumulating at the points of the attracting cycle.

To give an example of the supercritical center bifurcation of the fixed point R^* of the map F, we first present in Fig. 13 a 2D bifurcation diagram in the (δ_R, τ_R)-parameter plane at $\tau_L = 0.4, \delta_L = 0.5$ (for such parameter values the virtual fixed point $\overline{L}^*$ is an attracting focus; F is invertible), in which the regions of existence of the attracting cycles of different periods $n \leq 31$ are shown by different colors; the gray region corresponds to the divergent trajectories and the white region is related either to the attracting cycles of higher periodicity, or to chaotic attractors.

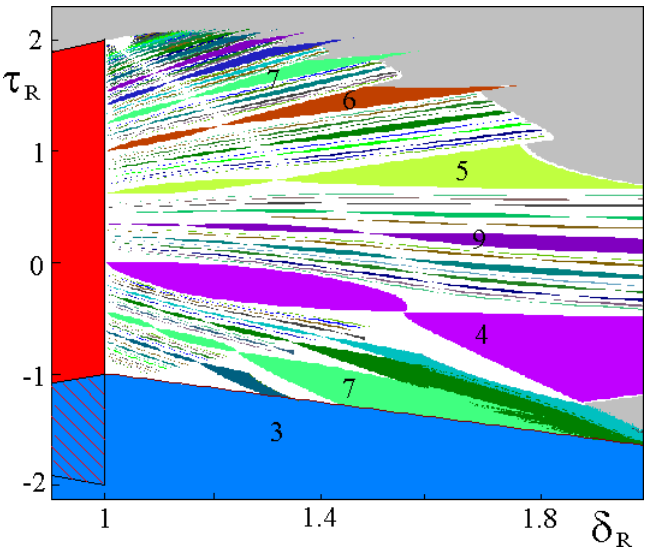

Fig. 13. 2D bifurcation diagram in the (δ_R, τ_R)-parameter plane at $\tau_L = 0.4, \delta_L = 0.5$.

The bifurcation structure of the (δ_R, τ_R)-parameter plane in case $(\tau_L, \delta_L) \in S(L^*)$ has been studied in detail (see [Sushko & Gardini, 2008]). Recall, in particular, that near the center bifurcation line $\delta_R = 1$ the periodicity regions (corresponding to the attracting cycles born due to the center bifurcation) are organized in a way similar to the Arnold tongues (being ordered according to the Farey summation rule), but differently from the smooth case the boundary curves of the periodicity regions, issuing from the line $\delta_R = 1$, correspond not to the standard saddle-node bifurcation but to the so-called "saddle-node" BCB (not related to an eigenvalue 1) at which the points of the related attracting and saddle cycles merge in pairs at the critical lines of related ranks, and after the bifurcation such cycles disappear. Without going into further details we just present in Fig. 14 an example of the closed invariant attracting curve $\mathcal{C}$ existing in the phase plane at $\tau_L = 0.4, \delta_L = 0.5, \tau_R = 0.62, \delta_R = 1.01$; this curve is born due the supercritical center bifurcation, and it is formed by the closure of the unstable set of the saddle 5-cycle approaching points of the attracting 5-cycle.

The bifurcation structure of the (δ_R, τ_R)-parameter plane in case $(\tau_L, \delta_L) \notin S(L^*)$, has not yet been studied in detail. We leave its systematic analysis for future work, but in the context of the present paper this case is interesting because for such parameter values we can find examples of *subcritical* center bifurcation of the fixed point R^*, as

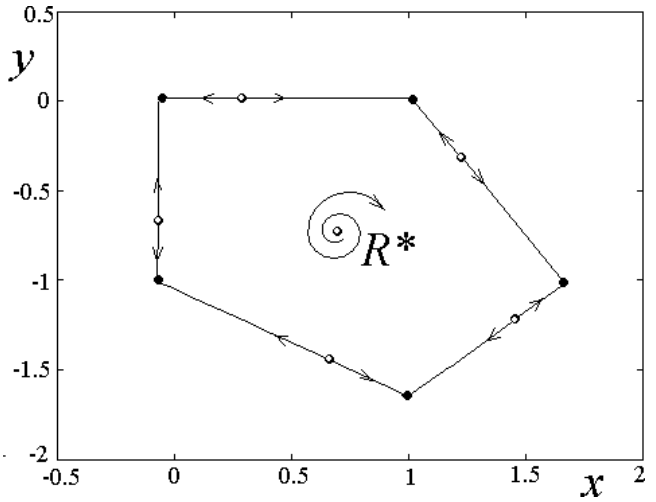

Fig. 14. Closed invariant attracting curve $\mathcal{C}$ at $\tau_L = 0.4, \delta_L = 0.5, \tau_R = 0.62, \delta_R = 1.01$.

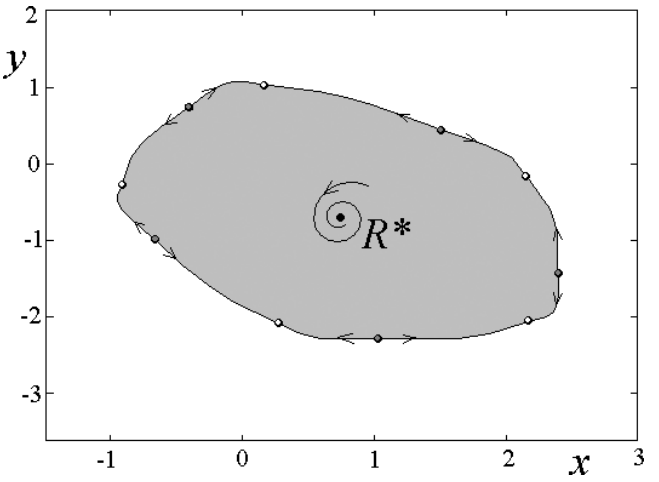

Fig. 15. The repelling closed invariant curve $\mathcal{C}$ in the case of rotation number 1/5 at $\tau_L = 0.62, \delta_L = 1.15, \tau_R = 0.62, \delta_R = 0.96$; the white (respectively grey) circles are the points of the saddle (respectively repelling node) cycle of period 5; R^* is an attracting focus.

well as of center bifurcation leading to a chaotic attractor.

As it was already mentioned, the invariant region ($P_{m/n}$ or Q) exists in the phase space of F at $\delta_R = 1, \tau_R \in (-2, 2)$ independently on the values of δ_L and τ_L. To get an example of the subcritical center bifurcation we need to find parameter values such that the fixed point R^* is an attracting focus (that holds for $\tau_R^2/4 < \delta_R < 1$), surrounded by a repelling closed invariant curve $\mathcal{C}$ which at $\delta_R = 1$ becomes the boundary of the invariant region ($P_{m/n}$ or Q) and for $\delta_R > 1$ disappears leaving the unstable focus. So, let $\tau_R^2/4 < \delta_R < 1$. To get the repelling closed invariant curve $\mathcal{C}$ formed by the stable set of a saddle k-cycle issuing from the points of a repelling k-cycle, we obviously need to have $|\delta_L| > 1$ (otherwise, if the determinants of both maps F_L and F_R are such that $|\delta_L| < 1$ and $|\delta_R| < 1$, then the determinant of any composite map is also less than 1 in modulus, so we can have only attracting and saddle cycles). The simplest case is to consider a repelling focus $\overline{L}^*$ with the same rotation number as the attracting focus R^*. Figure 15 presents an example of the repelling closed invariant curve $\mathcal{C}$ for $m/n = 1/5$ at $\tau_L = 0.62, \delta_L = 1.15, \tau_R = 0.62, \delta_R = 0.96$. Such a curve is formed by the closure of the stable set of the saddle 5-cycle (the white circles in Fig. 15) issuing from the points of the repelling 5-cycle (the gray circles). The curve $\mathcal{C}$ separates the basin of attraction of R^* shown in gray, from the points whose trajectories go to infinity. As $\delta_R \to 1$ the shape of the curve $\mathcal{C}$ is modified and at $\delta_R = 1$, it becomes the boundary of the invariant polygon $P_{1/5}$ with five edges, which in this case is repelling. One more example of the repelling closed invariant curve $\mathcal{C}$ at $\tau_L = 1, \delta_L = 1.1, \tau_R = 0.62, \delta_R = 0.99$ is presented in Fig. 16. In such a case the curve is formed either by the closure of the stable set of a saddle cycle of some high period, or by the closure of a quasiperiodic trajectory.

4.3. *Degenerate bifurcations of the cycle of period* 3; *transition to chaos via center bifurcation*

Other examples of the present section are related to the degenerate bifurcations of an attracting cycle of

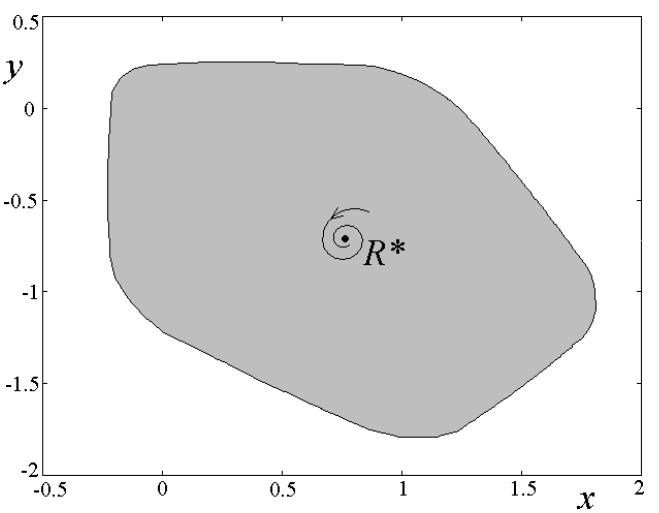

Fig. 16. The repelling closed invariant curve $\mathcal{C}$ at $\tau_L = 1, \delta_L = 1.1, \tau_R = 0.62, \delta_R = 0.99$.

period 3. Let $\gamma_3 = \{p_0, p_1, p_2\}$ be an attracting cycle of period 3 of the map F such that $p_0, p_1 \in L$ and $p_2 \in R$. Consider the region of existence and stability of the cycle γ_3 denoted $S(\gamma_3)$. The equations of the BCB boundaries of $S(\gamma_3)$ in the (δ_R, τ_R)-parameter plane at some fixed τ_L and δ_L are the following straight lines:

$$\begin{cases} \tau_R = \dfrac{\delta_R(1-\delta_L) - 1 - \tau_L}{\delta_L + \tau_L}, & \text{for } \delta_L \neq -\tau_L; \\ \delta_R = 1, & \text{for } \delta_L = -\tau_L; \end{cases} \qquad \text{BCB}_3^1 \tag{22}$$

$$\begin{cases} \tau_R = \dfrac{-\delta_R(\delta_L + \tau_L) + \delta_L - 1}{1 + \tau_L}, & \text{for } \tau_L \neq -1; \\ \delta_R = 1, & \text{for } \tau_L = -1. \end{cases} \qquad \text{BCB}_3^2 \tag{23}$$

It is not difficult to obtain also the equations defining the stability of γ_3. Indeed, the map F^3 corresponding to the considered cycle is $F^3 = F_R \circ F_L^2$, for which the related eigenvalues $\lambda_{1,2(\gamma_3)}$ are less than 1 in modulus for

$$\begin{cases} \begin{cases} \tau_R > \dfrac{\delta_R(\tau_L - \delta_L^2) - 1 + \delta_L\tau_L}{\tau_L^2 - \delta_L}, \\ \tau_R > \dfrac{\delta_R(\tau_L + \delta_L^2) + 1 + \delta_L\tau_L}{\tau_L^2 - \delta_L}, \end{cases} & \text{for } \tau_L^2 > \delta_L; \\ \begin{cases} \tau_R < \dfrac{\delta_R(\tau_L - \delta_L^2) - 1 + \delta_L\tau_L}{\tau_L^2 - \delta_L}, \\ \tau_R < \dfrac{\delta_R(\tau_L + \delta_L^2) + 1 + \delta_L\tau_L}{\tau_L^2 - \delta_L}, \end{cases} & \text{for } \tau_L^2 < \delta_L; \\ \delta_R < \dfrac{1}{\delta_L^2}, \end{cases}$$

so that the curve related to the DFB ($\lambda_{2(\gamma_3)} = -1$) is given by

$$\begin{cases} \tau_R = \dfrac{\delta_R(\tau_L - \delta_L^2) - 1 + \delta_L\tau_L}{\tau_L^2 - \delta_L}, & \text{for } \tau_L^2 \neq \delta_L; \\ \delta_R = \dfrac{\delta_L\tau_L - 1}{\delta_L^2 - \tau_L}, & \text{for } \tau_L^2 = \delta_L; \end{cases} \qquad \text{DFB}_3 \tag{24}$$

the curve related to the DTB ($\lambda_{1(\gamma_3)} = 1$) is given by

$$\begin{cases} \tau_R = \dfrac{\delta_R(\tau_L + \delta_L^2) + 1 + \delta_L\tau_L}{\tau_L^2 - \delta_L}, & \text{for } \tau_L^2 \neq \delta_L; \\ \delta_R = -\dfrac{\delta_L\tau_L + 1}{\delta_L^2 + \tau_L}, & \text{for } \tau_L^2 = \delta_L; \end{cases} \qquad \text{DTB}_3 \tag{25}$$

and the curve related to the center bifurcation (related to $|\lambda_{1,2(\gamma_3)}| = 1$ for the complex-conjugate $\lambda_{1,2(\gamma_3)}$) is given by

$$\delta_R = \frac{1}{\delta_L^2}, \quad \delta_L \neq 0. \quad \text{CB}_3. \tag{26}$$

Thus, at fixed $(\delta_L, \tau_L) \in S(L^*)$ in the (δ_R, τ_R)-parameter plane we have five straight lines such that each of them can be involved or not as a boundary of $S(\gamma_3)$ depending on δ_L and τ_L. It may also happen that $S(\gamma_3) = \varnothing$ as well as $S(\gamma_3)$ may be an unbounded set (as, for example, in the case $\delta_L = 0, \tau_L = 0.5$ such that in the (δ_R, τ_R)-parameter plane the boundaries of $S(\gamma_3)$ are the straight line $\text{BCB}_3^1, \text{BCB}_3^2$ and DFB_3, such that BCB_3^1 is parallel to DFB_3).

Note that the region $S(\gamma_3)$ shown in Fig. 13 in blue is overlapping with the stability region $S(R^*)$ of the fixed point R^* and with some other periodicity tongues (not indicated in this figure), in particular, with those issuing from the center bifurcation line $\delta_R = 1$ for $\tau_R < -1$. The two boundaries of $S(\gamma_3)$ shown in Fig. 13 are the BCB curves given in (22) and (23).

Now we give examples of the DFB of γ_3 and in the meantime we show that the center bifurcation of the fixed point R^* can lead to a chaotic attractor.

Let $\tau_L = -1.6, \delta_L = -0.9$ (for such parameter values the virtual fixed point $\overline{L}^*$ is a flip saddle, i.e. its eigenvalues have opposite sign). In Fig. 17 we show the (δ_R, τ_R)-parameter plane in which the straight lines $\text{BCB}_3^1, \text{BCB}_3^2, \text{DFB}_3, \text{DTB}_3$ and CB_3 (see (22)–(26)) are plotted, being the boundaries of the region $S(\gamma_3)$ (the dashed region) related to the existence and stability of the 3-cycle γ_3. Recall that γ_3 (having 2 points in L and 1 point in R) is born due to the BCB either at $(\delta_R, \tau_R) \in \text{BCB}_3^1$, or at $(\delta_R, \tau_R) \in \text{BCB}_3^2$, together with another 3-cycle denoted γ_3' (having 1 point in L and 2 points in R); These two cycles exist for the parameter values above the BCB lines BCB_3^1 and BCB_3^2 and below

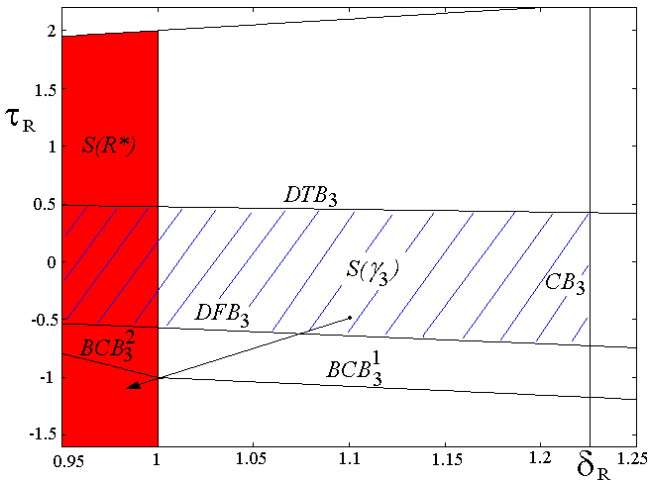

Fig. 17. The straight lines corresponding to the border-collision bifurcations ($\mathrm{BCB}_3^1, \mathrm{BCB}_3^2$) and the degenerate bifurcations ($\mathrm{DFB}_3, \mathrm{DTB}_3$ and CB_3) of the 3-cycle γ_3 at $\tau_L = -1.6, \delta_L = -0.9$.

DTB_3, moreover, the cycle γ_3 is a flip saddle for the parameter values below DFB_3.

Now let us take the $(\delta_R, \tau_R) \in S(\gamma_3)$, for example, $\delta_R = 1.1, \tau_R = -0.5$, and move the parameter point towards $(\delta_R, \tau_R) = (1, -1)$ (the related parameter path, indicated in Fig. 17 by the straight line with an arrow, is given by $\tau_R = 5\delta_R - 6$ for $\delta_R \in [0.99, 1.1]$). In Fig. 18 we present the corresponding 1D bifurcation diagram in the $(\delta_R, (x+y)/2)$-plane (note that there is another coexisting attractor for the same parameter values, which is not shown here, but some examples of such attractor will be presented later). In Fig. 18 we use the projection of the

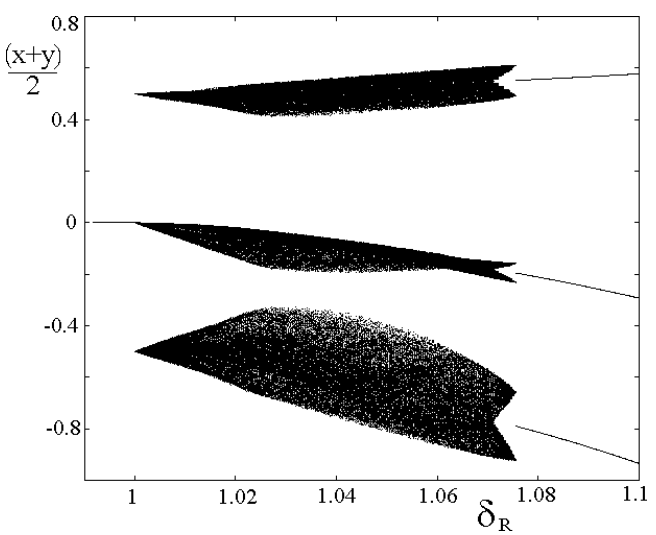

Fig. 18. 1Dim bifurcation diagram of the map F for $\delta_R \in (0.99, 1.1), \tau_R = 5\delta_R - 6, \tau_L = -1.6, \delta_L = -0.9$ (the straight line with an arrow in Fig. 17).

trajectory to the diagonal $y = x$ versus δ_R, instead of more standard projection either to x-, or to y-axes, in order to avoid overlapping branches of the attractor.

Let us comment the bifurcation sequence occurring when the parameter point follows the path indicated in Fig. 17 starting from the value $\delta_R = 1.1$, at which F has the attracting and saddle cycles γ_3 and γ_3'. For the parameter values corresponding to the intersection point of DFB_3 and our parameter path ($\delta_R \approx 1.076, \tau_R \approx -0.622$, see Fig. 17), for which the cycle γ_3 undergoes the DFB, in the (x, y)-plane there exist three segments denoted $S_i, i = 1, 2, 3$, each point of which, except the points of γ_3, is periodic of period 6: See Fig. 19 at which the segments S_i are shown being the local invariant sets of the points of γ_3, related to the eigenvalue -1; the stable invariant set of the saddle cycle γ_3' is also plotted as a boundary of the basin of attraction of the coexisting chaotic attractor. So, the cycle γ_3 undergoes the DFB giving rise to the cyclical chaotic attractors G_6 of period 6 (see an example in Fig. 20).

We continue to decrease the value of δ_R, and at $\delta_R \approx 1.0723$ the first homoclinic bifurcation of γ_3 occurs which results in pairwise merging of the pieces of G_6, giving rise to the cyclical chaotic attractor G_3 of period 3 (an enlarged piece of G_3 is shown in Fig. 21(a) together with stable invariant set of a point of γ_3 approximately at the moment

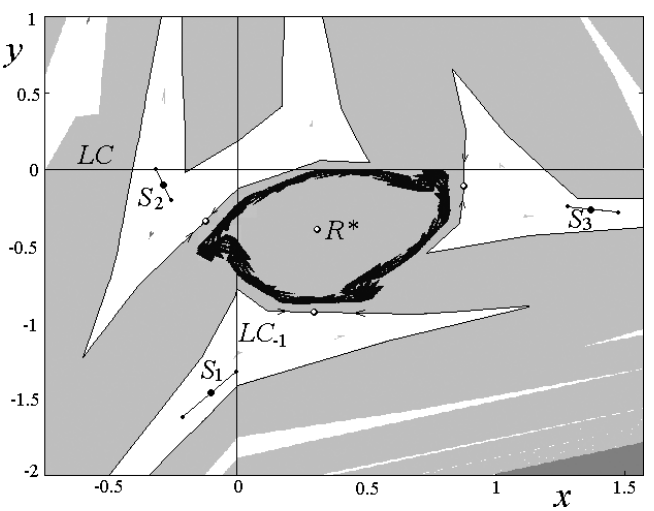

Fig. 19. The phase portrait of the map F at the parameter values related to the DFB of $\gamma_3 : \tau_L = -1.6, \delta_L = -0.9, \delta_R = 1.075596, \tau_R = -0.622019$. The segments S_i are the local invariant sets of the points of γ_3, related to the eigenvalue -1; The invariant stable set of the saddle cycle γ_3' gives the boundary separating the basins of the two coexisting attractors.

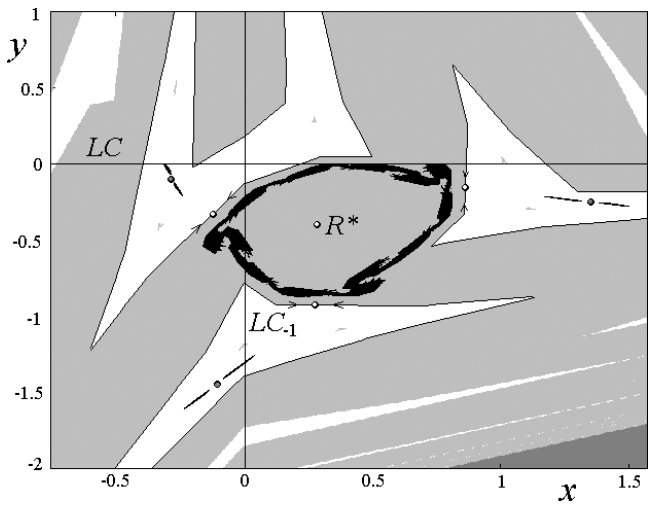

Fig. 20. The phase portrait of F at $\tau_L = -1.6, \delta_L = -0.9, \delta_R = 1.073, \tau_R = -0.635$. Here two chaotic attractors coexist: The 6-cyclical chaotic attractor G_6 born after the DFB of the cycle γ_3 and the one-piece chaotic attractor G_1.

of the first homoclinic bifurcation of γ_3). The next bifurcation is the transition $G_3 \Rightarrow G_6$ (which cannot be seen in the 1D bifurcation diagram in Fig. 18 due to the overlapping pieces of G_6), occurring as a result of the last homoclinic bifurcation of γ_3 at $\delta_R \approx 1.02865$ (see Fig. 21(b)). Note that the stable set of the saddle cycle γ_3' remains a separator of the basin of attraction of the considered attractors G_6 and G_3 from the basin of attraction of another coexisting attractor, while the basin of the points whose trajectories go to infinity is separated by the stable set of a saddle cycle of period 2.

At $\delta_R \to 1$ the pieces of G_6 tend in pair one to another, decreasing in size without merging, and at $\delta_R = 1$ they finally merge forming the 3-cycle which defines the vertexes of the invariant triangle $P_{1/3}$, while the cycle γ_3' becomes one of infinitely many 3-cycles belonging to the edges of $P_{1/3}$. Thus we have the center bifurcation of R^* (considered in the reverse order). Note that at $\delta_R = 1$ the second coexisting chaotic attractor undergoes the boundary crises.

Summarizing, the following bifurcation sequence can be observed if the (δ_R, τ_R)-parameter point follows the path indicated in Fig. 17 at $\tau_L = -1.6$, $\delta_L = -0.9$:

$$\gamma_3 \overset{\text{DFB}}{\Rightarrow} G_6 \overset{1^{st}\ \text{Hom}\ \gamma_3}{\Rightarrow} G_3 \overset{2^{nd}\ \text{Hom}\ \gamma_3}{\Rightarrow} G_6 \overset{\text{Center}\ B}{\Rightarrow} R^*.$$

4.3.1. *Center bifurcation of the 3-cycle*

To end this subsection we consider also an example of center bifurcation of the cycle γ_3 occurring when the (δ_R, τ_R) -parameter point crosses the center bifurcation line CB_3 given in (26) (see Fig. 17). Recall that $\gamma_3 = \{p_0, p_1, p_2\}$ is such that $p_0, p_1 \in L$ and $p_2 \in R$, so, the center bifurcation of γ_3 obviously corresponds to the center bifurcation of the fixed point p_0 of the map $F^3 = F_L^2 \circ F_R$ (or, of the fixed points p_1, p_2 of the maps $F_L \circ F_R \circ F_L, F_R \circ F_R^2$, respectively). So, we can apply the results obtained for the center bifurcation of the fixed point R^*: In particular, at the center bifurcation parameter values in the phase plane of the map F there exist

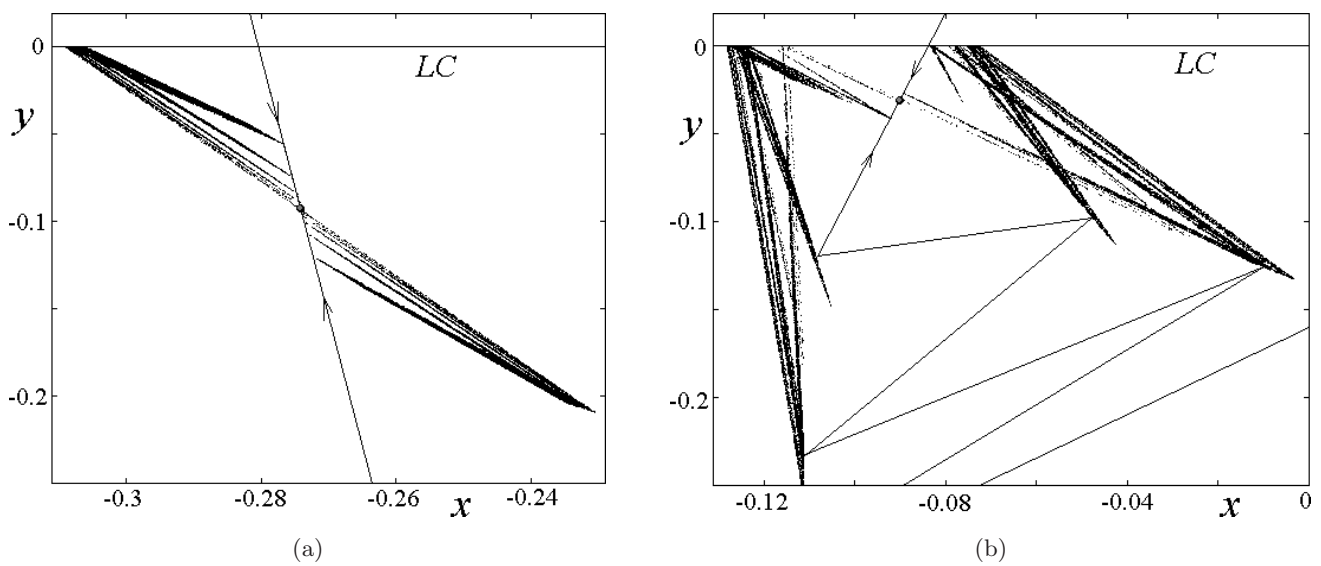

(a) (b)

Fig. 21. Enlargement of the phase space of the map F, showing one of the three parts of the cyclical attractor. The first (a) and the last (b) homoclinic bifurcations of γ_3, occurring, respectively, at $\delta_R \approx 1.0723$ and $\delta_R \approx 1.02865$. Here $\tau_L = -1.6, \delta_L = -0.9, \tau_R = 5\delta_R - 6$.

3-cyclical regions invariant under the proper composite map F^3. For an irrational rotation number each of the regions is bounded by an F^3-invariant ellipse tangent to the critical lines of proper ranks, while for a rational rotation number m/n there exist 3-cyclical F^3-invariant polygons denoted $P^{(i)}_{m/n}, i = 1, 2, 3$, each of which has n edges which are proper segments of the critical lines of the related ranks.

Let, as before, $\tau_L = -1.6, \delta_L = -0.9$ (see Fig. 17) and let $\delta_R = 1/\delta_L^2$. It is not difficult to obtain the value of τ_R related to the rotation number m/n: We write down the eigenvalues $\lambda_{1,2(\gamma_3)}$ of F^3 and solve the equation $\mathrm{Re}\,\lambda_{1,2} = \cos(2\pi m/n)$ with respect to τ_R :

$$\tau_R = \tau_{R,m/n} = \frac{2\cos\left(\dfrac{2\pi m}{n}\right) + \tau_L(\delta_L + \delta_R)}{\tau_L^2 - \delta_L}; \quad (27)$$

(note that we have to consider $\tau_R^* < \tau_R < \tau_R^{**}$, where the values τ_R^*, τ_R^{**} correspond to the intersection points of CB_3 with DFB_3 and DTB_3). For example, at $\tau_R = \tau_{R,1/6} \approx 0.1343, \delta_R = 1/\delta_L^2 \approx 1.2346$, in the phase plane of F there exist three cyclical F^3-invariant polygons $P^{(i)}_{1/6}, i = 1, 2, 3$, with six edges, each point of which, except the points of γ_3, is periodic of period 18.

Figure 22 presents the phase portrait of the map F at $\tau_L = -1.6, \delta_L = -0.9, \delta_R = 1/\delta_L^2, \tau_R = \tau_{R,1/6}$: the polygons $P^{(i)}_{1/6}, i = 1, 2, 3$, are shown in dark grey; the basin of attraction of the chaotic attractor shown in light grey, is bounded by the stable invariant set of the saddle cycle γ_3', moreover, it can be seen that this attractor is at the moment of its contact bifurcation (or, in other words, boundary crises), which occurs due to the first homoclinic bifurcation of γ_3', and if we increase δ_R a little bit the chaotic attractor will disappear leaving a chaotic repellor.

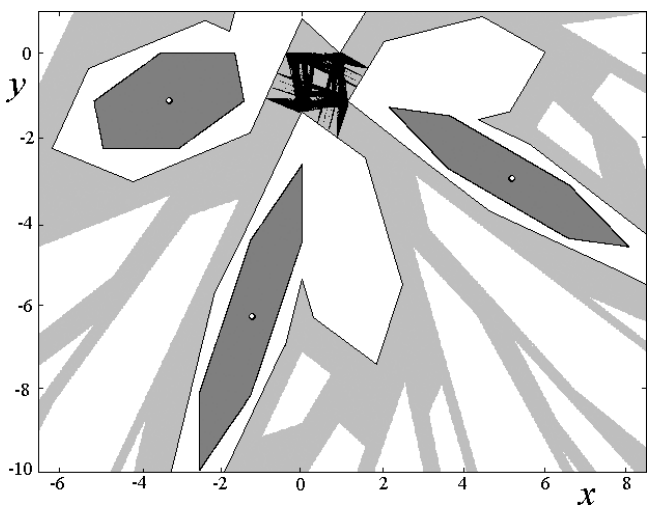

Fig. 22. The phase portrait of F at $\tau_L = -1.6, \delta_L = -0.9, \delta_R = 1/\delta_L^2, \tau_R = \tau_{R,1/6}$ given in (27), related to the center bifurcation of the cycle γ_3: there exist three polygons (invariant for F^3) with six edges shown in dark grey, each point of which is periodic of period 18.

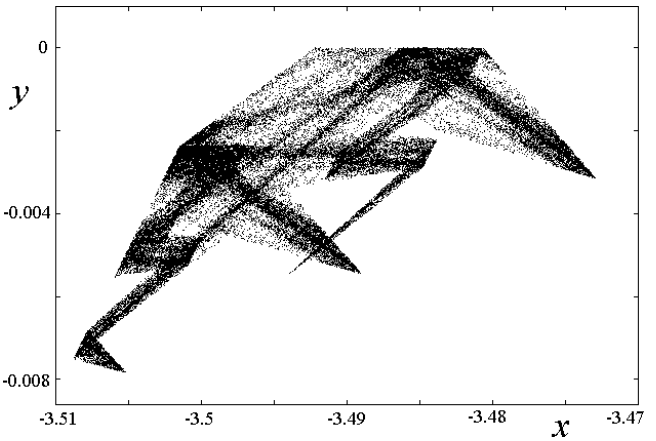

Fig. 23. An enlarged piece of 18-cyclical chaotic attractor at $\tau_L = -1.6, \delta_L = -0.9, \delta_R = 1/\delta_L^2 + 0.001, \tau_R = \tau_{R,1/6} - 0.001$.

The center bifurcation of γ_3 occurring for the considered parameter values leads to a cyclical chaotic attractor of period 18 (see Fig. 23 which presents an enlarged piece of such an attractor at $\tau_L = -1.6, \delta_L = -0.9, \delta_R = 1/\delta_L^2 + 0.001, \tau_R = \tau_{R,1/6} - 0.001$).

Acknowledgments

The authors are indebted to Viktor Avrutin for his help in determining some homoclinic bifurcation curves via numerical simulations.

References

Avrutin, V. & Schanz, M. [2006] "Multi-parametric bifurcations in a scalar piecewise-linear map," *Nonlinearity* **19**, 531–552.

Avrutin, V., Schanz, M. & Gardini, L. [2009a] "On a special type of border-collision bifurcations occurring at infinity," submitted for publication.

Avrutin, V., Schanz, M. & Gardini, L. [2009b] "Calculation of bifurcation curves by map replacement," submitted for publication.

Banerjee, S. & Grebogi, C. [1999] "Border-collision bifurcations in two-dimensional piecewise smooth maps," *Phys. Rev. E* **59**, 4052–4061.

Banerjee, S., Karthik, M. S., Yuan, G. & Yorke, J. A. [2000a] "Bifurcations in one-dimensional piecewise

smooth maps — Theory and applications in switching circuits," *IEEE Trans. Circuits Syst.-I: Fund. Th. Appl.* **47**, 389–394.

Banerjee, S., Ranjan, P. & Grebogi, C. [2000b] "Bifurcations in two-dimensional piecewise smooth maps — Theory and applications in switching circuits," *IEEE Trans. Circuits Syst.-I: Fund. Th. Appl.* **47**, 633–643.

De Melo, W. & van Strien, S. [1993] *One-Dimensional Dynamics* (Springer, NY).

di Bernardo, M., Feigin, M. I., Hogan S. J. & Homer, M. E. [1999] "Local analysis of C-bifurcations in n-dimensional piecewise smooth dynamical systems," *Chaos Solit. Fract.* **10**, 1881–1908.

di Bernardo, M., Budd, C. J., Champneys, A. R. & Kowalczyk, P. [2008] *Piecewise-Smooth Dynamical Systems Theory and Applications* (Springer-Verlag, London).

Feely, O., Fournier-Prunaret, D., Taralova-Roux, I. & Fitzgerald, D. [2000] "Nonlinear dynamics of bandpass sigma-delta modulation. An investigation by means of the critical lines tool," *Int. J. Bifurcation and Chaos* **10**, 303–327.

Feigin, M. I. [1970] "Doubling of the oscillation period with C-bifurcations in piecewise-continuous systems," *Prikl. Math. Mekh.* **34**, 861–869 (in Russian).

Fournier-Prunaret, D., Feely, O. & Taralova-Roux, I. [2001] "Lowpass sigma-delta modulation: An analysis by means of the critical lines tool," *Nonlin. Anal.* **47**, 5343–5355.

Fournier-Prunaret, D., Charge, P. & Gardini, L. [2008] "Bifurcations in a 2D piecewise-smooth map modeling a switching circuit," DIFF-2008 Suzdal, Russia.

Gallegati, M., Gardini, L., Puu, T. & Sushko, I. [2003] "Hicks' trade cycle revisited: Cycles and bifurcations," *Math. Comput. Simul.* **63**, 505–527.

Gardini, L., Sushko, I. & Naimzada, A. [2008] "Growing through chaotic intervals," *J. Econ. Th.* **143**, 541–557.

Gardini, L., Avrutin, V. & Schanz, M. [2009a] "Connection between bifurcations on the Poincarè Equator and the dangerous bifurcations," *Grazer Mathematische Berichte*, to appear.

Gardini, L., Tramontana, F., Avrutin, V. & Schanz, M. [2009b] "Border collision bifurcations in 1D PWL map and the Leonov approach," submitted for publication.

Guckenheimer, J. & Holmes, P. [1983] *Nonlinear Oscillations, Dynamical Systems, and Bifurcations of Vector Fields* (Springer-Verlag, NY).

Halse, C., Homer, M. & di Bernardo, M. [2003] "C-bifurcations and period-adding in one-dimensional piecewise-smooth maps," *Chaos Solit. Fract.* **18**, 953–976.

Ito, S., Tanaka, S. & Nakada, H. [1979] "On unimodal transformations and chaos II," *Tokyo J. Math.* **2**, 241–259.

Kocic, V. L. & Ladas, G. [1993] *Global Behavior of Nonlinear Difference Equations of Higher Order with Applications* (Kluwer Academic Publishers).

Kuznetsov, Y. A. [1998] *Elements of Applied Bifurcation Theory* (Springer-Verlag, NY).

Leonov, N. N. [1959] "Map of the line onto itself," *Radiofisika* **3**, 942–956.

Lozi, R. [1978] "Un attracteur étrange du type attracteur de Hénon," *J. Phys. Colloque* C5 **39**, supplément au no. 8, 9–10.

Maistrenko, Y. L., Maistrenko, V. L. & Chua, L. O. [1993] "Cycles of chaotic intervals in a time-delayed Chua's circuit," *Int. J. Bifurcation and Chaos* **3**, 1557–1572.

Maistrenko, Y. L., Maistrenko, V. L., Vikul, S. I. & Chua, L. O. [1995] "Bifurcations of attracting cycles from time-delayed Chua's circuit," *Int. J. Bifurcation and Chaos* **5**, 653–671.

Maistrenko, Y., Sushko, I. & Gardini, L. [1998] "About two mechanisms of reunion of chaotic attractors," *Chaos Solit. Fract.* **9**, 1373–1390.

Mira, C., Gardini, L., Barugola, A. & Cathala, J. C. [1996] *Chaotic Dynamics in Two-Dimensional NonivertibIe Maps*, Nonlinear Sciences, Series A (World-Scientific, Singapore).

Nusse, H. E. & Yorke, J. A. [1992] "Border-collision bifurcations including period two to period three for piecewise smooth systems," *Physica D* **57**, 39–57.

Nusse, H. E. & Yorke, J. A. [1995] "Border-collision bifurcation for piecewise smooth one-dimensional maps," *Int. J. Bifurcation and Chaos* **5**, 189–207.

Puu, T. & Sushko, I. [2002] *Oligopoly Dynamics, Models and Tools* (Springer Verlag, NY).

Puu, T. & Sushko, I. [2006] *Business Cycle Dynamics, Models and Tools* (Springer Verlag, NY).

Sharkovsky A. N., Kolyada, S. F., Sivak, A. G. & Fedorenko, V. V. [1997] *Dynamics of One-Dimensional Maps* (Kluwer Academic, Boston).

Simpson, D. J. W. & Meiss, J. D. [2008] "Neimark–Sacker bifurcations in planar, piecewise-smooth, continuous maps," *SIAM J. Appl. Dyn. Syst.* **7**, 795–824.

Sushko, I., Maistrenko, Y. & Gardini, L. [1999] "On chaotic attractors at the transition from homeomorphism to endomorphism in a family of two-dimensional maps," *Grazer Math. Ber.* **339**, 335–346.

Sushko, I., Puu, T. & Gardini, L. [2003] "The Hicksian floor-roof model for two regions linked by interregional trade," *Chaos Solit. Fract.* **18**, 593–612.

Sushko, I., Agliari, A. & Gardini, L. [2005] "Bistability and border-collision bifurcations for a family of unimodal piecewise smooth maps," *Discr. Contin. Dyn. Syst. Serie B* **5**, 881–897.

Sushko, I., Agliari, A. & Gardini, L. [2006] "Bifurcation structure of parameter plane for a family of unimodal piecewise smooth maps: Border-collision bifurcation curves," *Dynamic Modelling in Economics*

and Finance in Honour of Professor Carl Chiarella, eds. Bischi, G. I. & Sushko, I., *Chaos Solit. Fract.* **29**, 756–770.

Sushko, I. & Gardini, L. [2008] "Center bifurcation for two-dimensional border-collision normal form," *Int. J. Bifurcation and Chaos* **18**, 1029–1050.

Sushko, I. & Gardini, L. [2009] "Center bifurcation of a point on the Poincaré equator," *Grazer Mathematische Berichte*, to appear.

Takens, F. [1987] "Transitions from periodic to strange attractors in constrained equations," in *Dynamical Systems and Bifurcation Theory*, eds. Camacho, M. I., Pacifico, M. J., Takens, F., Pitman Research Notes in Mathematics Series, Vol. 160 (Longman Scientific and Techical), pp. 399–421.

Tramontana, F., Gardini, L. & Puu, T. [2008] "Duopoly games with alternative technologies," *J. Econ. Dyn. Contr.* **33**, 250–265.

Zhusubaliyev, Z. T. & Mosekilde, E. [2003] *Bifurcations and Chaos in Piecewise-Smooth Dynamical Systems* (World Scientific, Singapore).

Zhusubaliyev, Z. T., Mosekilde, E., Maity, S., Mohanan, S. & Banerjee, S. [2006] "Border collision route to quasiperiodicity: Numerical investigation and experimental confirmation," *Chaos* **16**, 1–11.